Review

Recent progress in blue energy harvesting for powering distributed sensors in ocean

Tiancong Zhao [a,b,c,1], Minyi Xu [a,*,1], Xiu Xiao [a,1], Yong Ma [b,c], Zhou Li [d,*], Zhong Lin Wang [d,e,**]

[a] Marine Engineering College, Dalian Maritime University, Dalian 116026, China
[b] School of Marine Engineering and Technology, Sun Yat-sen University, Guangzhou 510275, China
[c] Southern Marine Science and Engineering Guangdong Laboratory (Zhuhai), Zhuhai 519000, China
[d] CAS Center for Excellence in Nanoscience, Beijing Key Laboratory of Micro-nano Energy and Sensor, Beijing Institute of Nanoenergy and Nanosystems, Chinese Academy of Sciences, Beijing 101400, China
[e] School of Materials Science and Engineering, Georgia Institute of Technology, Atlanta, GA 30332-0245, United States

ARTICLE INFO

ABSTRACT

Oceanography has received a lot of attention in the 21st century. Due to the harsh and complex ocean conditions, ensuring power supply to the distributed marine equipment has become a critical challenge. The ocean kinetic energy harvester (OKEH) has made favorable progress in powering ocean sensors by harvesting blue energy. The latest developments in the electromagnetic harvester (EMH), electroactive polymers harvester (EAH), triboelectric nanogenerator (TENG), and hybrid harvester (HH) are reviewed in this study. This study analyzes the working principles and output performance of the OKEH as well as highlights the future challenges of and perspectives on the OKEH. Based on the comparison of OKEHs, this study indicates that TENG is favorable for harvesting low-frequency, low-amplitude, and random-direction wave energy (called high entropy energy).

1. Introduction

With ocean development and utilization, ocean environmental pollution and natural disasters have gradually increased, causing enormous economic losses and social impacts [1]. Ocean monitoring and the remote control of various marine equipment are the most popular approaches for solving these problems [2]. Ocean sensor is the most essential equipment for collecting data and transferring control signals from distant places, and a large number of ocean distributed sensors form the basis of ocean monitoring [1–14]. As an extension of the Internet of Things (IoT), sensing the ocean is playing an increasingly vital role in developing smart oceans [2,3,15].

As shown in Fig. 1, smart ocean consists of many ocean sensors and unmanned equipment. Deployed on floating bodies or along cables,

energy harvesters can convert wave, solar, wind, tidal, ocean current, and other renewable energy sources to stable electrical energy. Ocean sensors are the basis for underwater sensor networks (UWSNs) and wireless sensor networks (WSNs) [2, 11–13, 16–24]. The UWSNs can be integrated with ships, cargos, buoys, underwater equipment, and offshore platforms to collect information and transmit it over the internet [19,23]. By supplementing machine learning and multi-sensor fusion techniques, the ocean sensors can collect data from the marine environment, perform pollution monitoring, and analyze the in-situ water quality in detail. In addition, ocean sensors have a great potential in marine channel safety, ship navigation, marine monitoring, and resource protection [2,3]. At this stage, the miniature electronic product like Micro-Electro-Mechanical System opens up many opportunities for low-power sensors [25]. Sensor-based ocean monitoring equipment has

---

been developed in the recent years [2, 8, 10, 26–30]. However, the complexity of the marine environment and limited battery capacity have led to the serious lack of intelligent and convenient marine exploration facilities [16,17].

The main compositions of the state-of-the-art ocean sensors have been briefly illustrated in Fig. 2. The main aim nowadays is to enable sensor nodes to operate in oceans for a long time [11,31]. The energy supply for sensor nodes usually includes batteries, capacitors, heat engines, fuel cells, and energy harvesters. In the past decades, battery power has been the most commonly used energy source [11]. However, with the rapid increase in the number and scale of sensor networks, the replacement of the exhausted batteries has become significantly time-consuming and laborious [3,5,31]. In addition, the batteries often involve toxic heavy metals and is not conducive to the development of the marine ecological environment.

Ocean sensors face several chemical, physical, and biological effects. There are over 4000 organisms related to fouling problems in the marine environment [13, 17, 56–60]. Once the ocean sensors immerse in seawater, they cause biofouling problems and influence various aspects of the seawater, such as, pH, dissolved oxygen, temperature, conductivity, organic material, and hydrodynamic conditions. Consequently, the long-term accuracy of the marine environmental sensor measurements has been a critical issue [2]. The control of biofouling of surfaces in the marine environment is a considerable challenge has detrimental effects on shipping, oceanographic sensors and aquaculture systems. For example, it has been shown that the increased roughness presented by a heavily fouled ship hull can result in powering penalties of up to 86% at cruising speed; even relatively light fouling by diatom 'slimes' can generate a 10–16% penalty [61,62]. Because seawater is corrosive, the oceanographic sensors should take appropriate fouling protection measures. The biofouling protection for ocean sensors includes three typical methods: wipers, copper corrosion, and chlorine evolution [17, 62–64]. However, it is difficult to conduct these methods in an actual ocean environment and therefore, the biofouling protection for oceanographic in-situ sensors is more challenging. With the existing technologies, the wide-scale deployment of ocean sensors is hindered. For an electrical equipment that requires distributed, low power consumption, and strong robustness, energy harvesting may be the most effective method [5,31,65,66].

Notably, the ocean is not only rich in natural resources, such as oil and gas, but also in potential energy. In 2014, Tollefson defined blue energy as the power from the ocean and stated that the sea could be an even more benign source of power than the wind [67]. Professor Wang considered blue energy as a clean, cost-effective, and sustainable energy sourced from the ocean [68]. Generally, blue energy indicates the energy obtained from ocean, while the devices that harvest energy from the ocean are called blue energy harvesters. In other words, the "regular" and "effective" energy collected by the power generation devices from the "irregular" ocean kinetic energy (OKE) can be categorized as blue energy. Blue energy typically offer two forms of kinetic energy, ocean currents and ocean waves [65]. Specifically, it is estimated that the average energy in the waves along the world coastline is approximately 65 MW per mile [65, 67, 69–73]. Representative of blue energy, OKE is characterized by its sustainability and reproducibility [65,67,74,75]. Fig. 3 shows the power density for various wave heights and current velocities of the OKE [76,77]. The wave power is proportional to the square of the wave height, and the current power is proportional to the cube of the current velocity. Therefore, OKE is a relatively intense renewable energy source and is favorable for powering distributed ocean sensors. Considering the low power requirements of ocean sensors, it is expected that the blue energy harvesters will provide a long-term and effective power supply for ocean sensors.

Recent progress in ocean energy utilization has shown that ocean kinetic energy harvesters (OKEH) and blue energy storage technologies are expected to replace the traditional batteries and cables. The converted energy can completely meet the requirements of small-scale and low-power electrical equipment, such as ocean sensors, as shown in Fig. 4. Further, it is possible to realize a long-term stable power supply for marine monitoring equipment.

2. Types of energy harvesters for powering distributed sensors

2.1. Characteristics of kinetic energy harvested from ocean

Waves are derived from the transfer of the kinetic energy of wind to the upper surface of ocean [78]. The obvious advantage of wave energy is that it can travel across a long distance without any significant energy loss. The power is steadier and more predictable, and it allows much
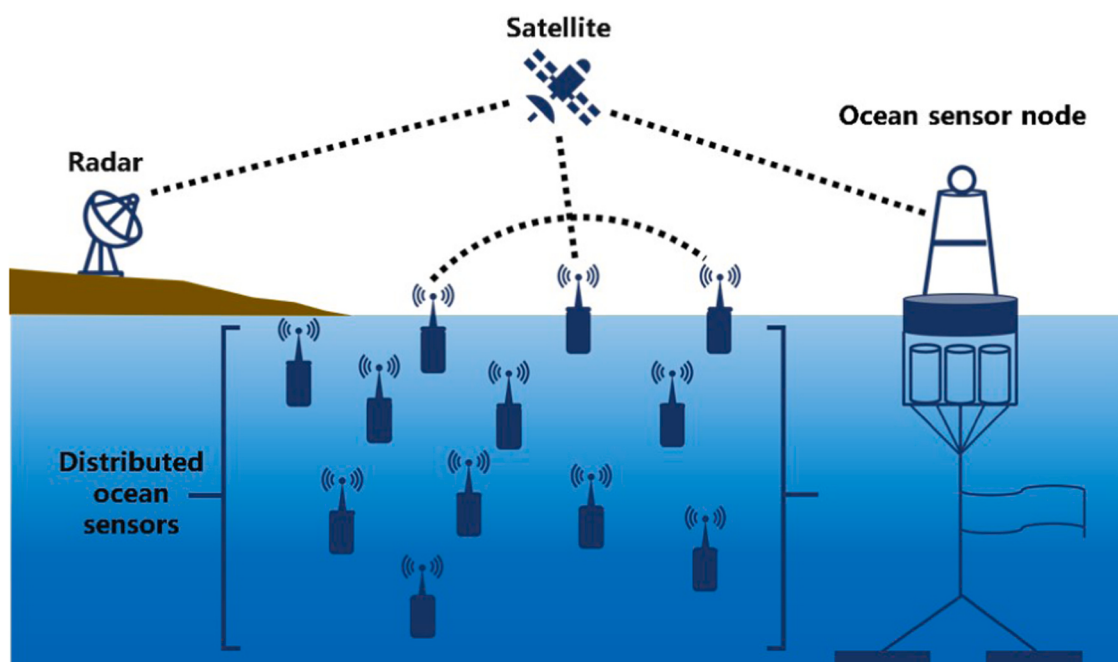

Fig. 1. Vast network of unmanned ocean systems and sensors for smart ocean.
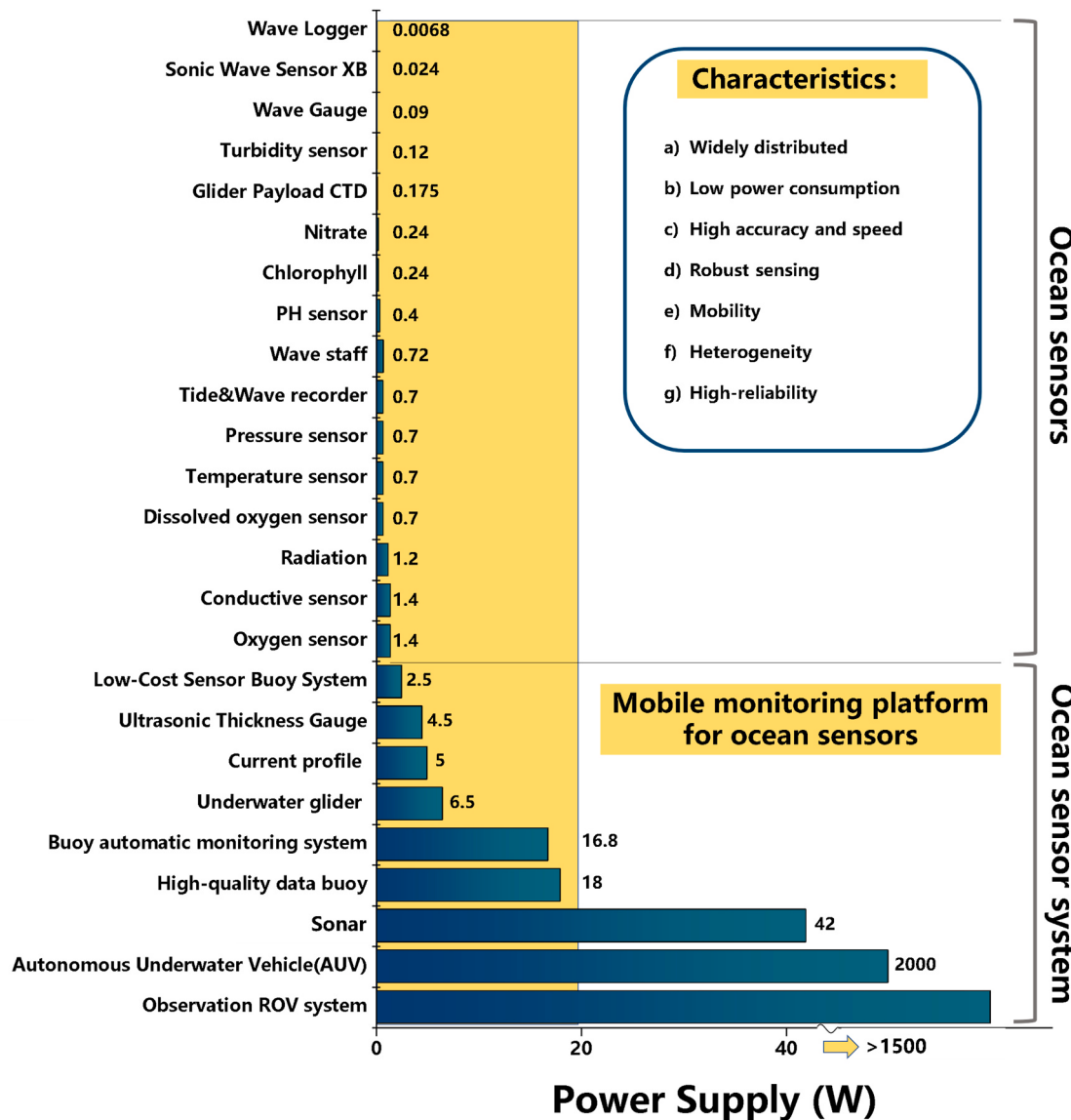
Fig. 2. State-of-art ocean sensors: Observation Remotely Operated Vehicle (ROV) system [32], Autonomous Underwater Vehicle (AUV) [20,33], Sonar sensors [34], High-quality data buoy [35], Buoy automatic monitoring system [36], Underwater glider [37], Current profile [38], Ultrasonic thickness gauge [39], Low-Cost sensor buoy system [26], Oxygen sensor [40], Conductive sensor [41], Radiation [42], Dissolved oxygen sensor [43], Temperature sensor [44], Pressure sensor [45], Tide and Wave recorder [46], Wave staff [47], pHsensor [48], Chlorophyll [49], Nitrate [50], Glider Payload CTD [51], Turbidity sensor [52], Wave gauge [53], Sonic wave sensor XB [54], and Wave logger [55].

smaller and fewer components to produce the same amount of power in certain regions [60, 69, 72, 79–82]. Kinetic energy in waves is tremendous. An average 4-ft, 10-s wave embodies an energy level greater than 35,000 horsepower per mile of coast [79]. The wave power per unit in deep water for a regular wave is given by,

$$J = \frac{1}{4} \frac{\rho (ga)^2 T}{2\pi} = \frac{\rho T (gH)^2}{32\pi}, \qquad (1)$$

where, ρ is the mass density of water, g is the acceleration of gravity, a is the wave amplitude, H is the wave height, and T is the period of the wave. From Eq. (1), it can be noted that the wave power is proportional to the square of the wave height and the square root of the wavelength and linearly proportional to the wave period.

As illustrated in Fig. 5, the current energy consists of tidal current and ocean current energy. The tidal current energy is produced from the gravitational pull from both the moon and the sun [83]. Tidal currents are the response of the ocean water mass to the tide and are generated by horizontal movements of water (particularly, near coasts or other

constrictions). An initial analysis of the tidal current resource can be done similar to the wind analysis [84],

$$P = \frac{1}{2} \rho \int \left(U^3 dA \right), \qquad (2)$$

where, ρ is the water density, A is the cross-sectional area of the channel (m^2), and U is the component of the undisturbed fluid flow velocity perpendicular to the cross-section of the channel (m/s) [84]. It can be seen that the potential power of a tidal current is proportional to the cube of the current velocity. Therefore, the power density (in W/m^2) of tidal currents increases substantially with a small increase in the velocity. For near-shore currents such as those occurring in the channels between mainland and islands or in estuaries, the current velocity varies predictably with respect to the tide [78]. Compared with the near-shore tidal current energy, significant current flows also exist in the open ocean [78]. These large circulations are initiated by the latitudinal distributions of winds, temperature, and salinity across the globe [85]. The ocean currents flow continuously in the same direction and is the
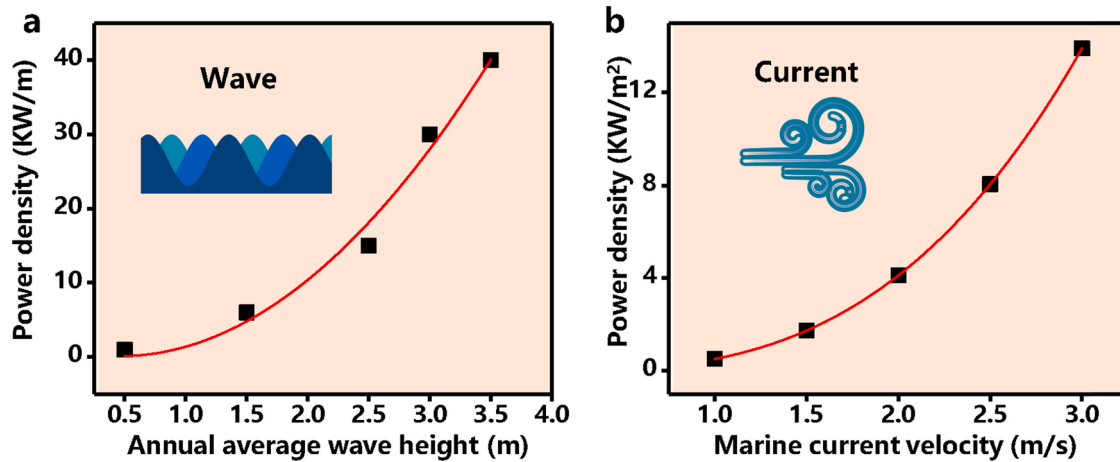
Fig. 3. Relative power density of (a) ocean wave with different wave heights and (b) marine current with different current velocities [76,77].
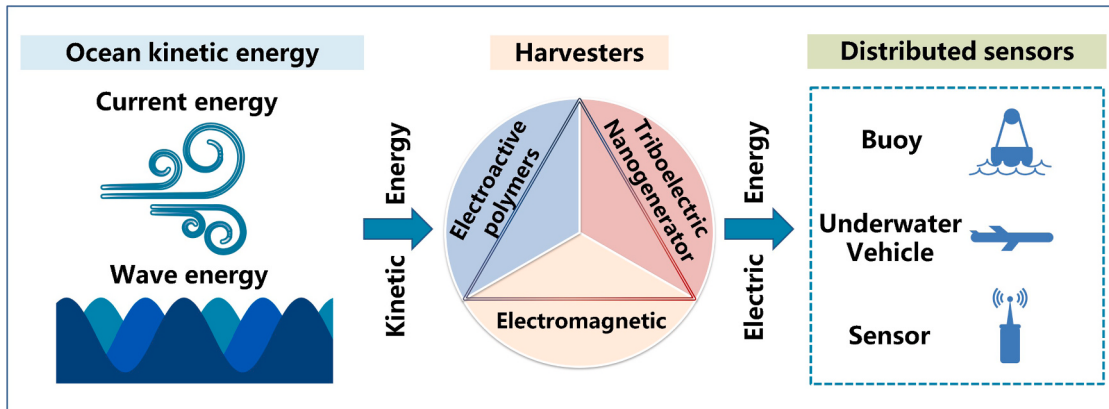

Fig. 4. Schematic of OKE harvesters for powering distributed sensors.

strongest, close to the surface.

The OKE resource zones comprising ocean wave energy resource zone, wave-current interaction zone, and marine current resource zone, are depicted in Fig. 5. The currents and wave-driven flows interact with the seabed, producing boundary layers. The ubiquitous presence of currents results in a turbulent bottom boundary layer with a thickness of the order of meters to a few tens of meters [86]. In addition, the waves produce a boundary layer only when the oscillatory motion extends to the seafloor, that is often the most turbulent, with a thickness of the order of 0.1 m [86]. The wave and current spectrum are prone to becoming highly irregular. Under the actual sea conditions, the waves, tidal currents, ocean currents, wind, and temperature interact with each other, making the associated energy conversion more chaotic and irregular. Based on the concept of entropy from the first law of thermodynamics, a large amount of irregular energy distributed in the ocean has a high entropy. It is further noted that, due to the influence of lunar cycle, wind, temperature, salinity, and gravity, the OKE is usually "random" (high entropy), and the parameters of the various marine environments affect the efficiency and accessibility of OKEHs [68,70, 87]. However, given only a small fraction of the OKE, the electricity demand of the distributed ocean sensors can be fulfilled [68].

Considering the wave and current resource characteristics, the OKE technology is still in the accelerating stage and is expected to grow rapidly in the next decade. OKEH has made significant progress in powering ocean sensors by harvesting blue energy. The latest developments in the electromagnetic harvesters (EMHs), electroactive polymers harvesters (EAHs), triboelectric nanogenerators (TENGs), and hybrid harvester (HHs) are comprehensively reviewed in the following

Section.

2.2. Electromagnetic harvesters

2.2.1. Working principle

Faraday's law of electromagnetic induction states that a varying magnetic field can induce electric current [70,74,88]. The traditional EMH is composed of a magnet and metal coil that usually yields a large volume, high mass density, and single acquisition direction. The basic principle is that the Lorentz force induces electrons to flow in a conductor, as shown in Fig. 6 [70]. In fact, the EMH has performed effectively in critical applications in large-scale ocean power stations and other ocean renewable energy utilization fields [20, 60, 69, 71, 72, 80–82, 89–99]. However, due to the "high-entropy" or "disorder" nature of the OKE, the traditional EMH is inefficient for powering small-scale appliances, such as distributed sensor nodes and ocean monitoring equipment [70,100,101]. Therefore, researchers have proposed numerous smaller-scale and more robust EMH-based renewable OKE harvesting technologies to power ocean sensors [96, 102–106].

2.2.2. Oscillating water column mode

As shown in Fig. 7 (a), Olly et al. proposed a wave energy harvester based on the oscillating water column (OWC) and is called the backward bent duct buoy (BBDB) [103]. The basic structure is composed of two interconnected L-shaped duct chambers which is kept immersed in water. The turbine is located between the two-duct connection ports. It uses buoys as the basic structure. When the BBDB is excited by waves, the water levels inside the two ducts are different, causing a pressure
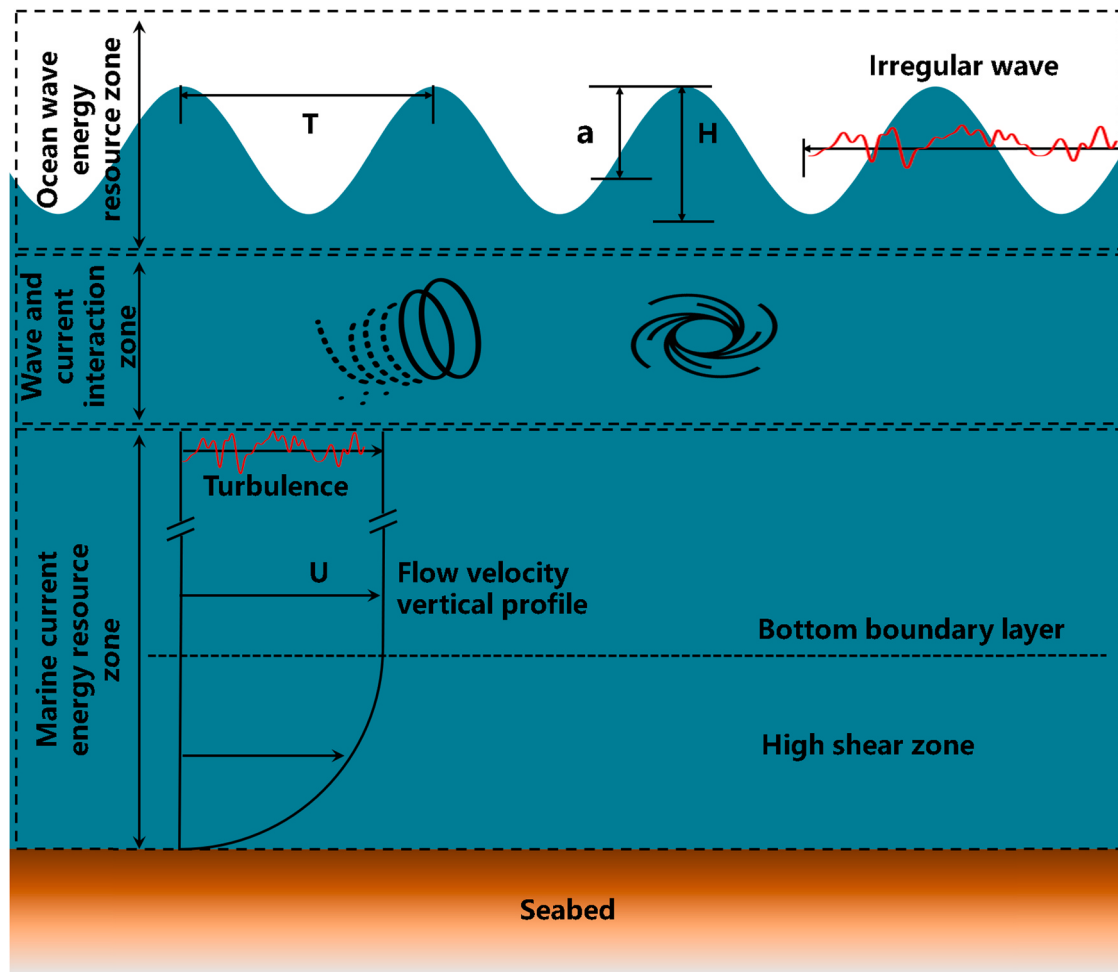
Fig. 5. Schematic diagram showing the characteristics and resource zone of OKE.
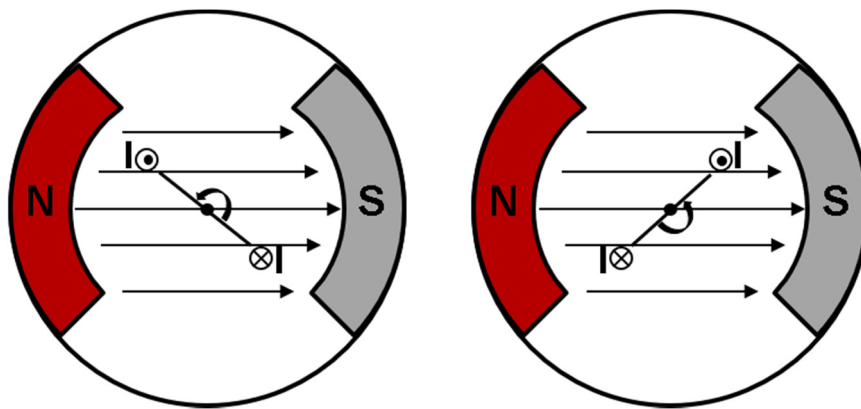
Fig. 6. Working mechanism of an electromagnetic harvester: a metal coil cuts through the magnetic induction lines generated by a magnet.

difference that drives the turbine to generate electricity. It affords the advantages of a high primary conversion efficiency and maximum conversion efficiency at the maximum wavelength. The maximum efficiency of BBDB is approximately 78% [Pw = 326.3725 (water power), avgPc = 255.04 (chamber power)] [103]. Upon applying the BBDB to marine ranches, the aquaculture monitoring system can operate stably [103].

2.2.3. Inertial pendulum mode

Ding et al. proposed an inertial pendulum OKEH for powering sensors in an underwater glider [105]. It consists of an eccentric pendulum fixed with a rare earth permanent magnet generator. Under wave excitations, the eccentric pendulum rotates around the center, causing the coil to produce electricity in the changing magnetic field. Therefore, it does not require any gear set and can directly convert blue energy into electricity. In the first-level sea state, the average power is greater than 150 mW, sufficient for providing power to a large number of sensors [105].

Li et al. proposed an OKEH based on the high-efficiency pendulum, as shown in Fig. 8 (a) [102]. The pendulum can sense the motion of the
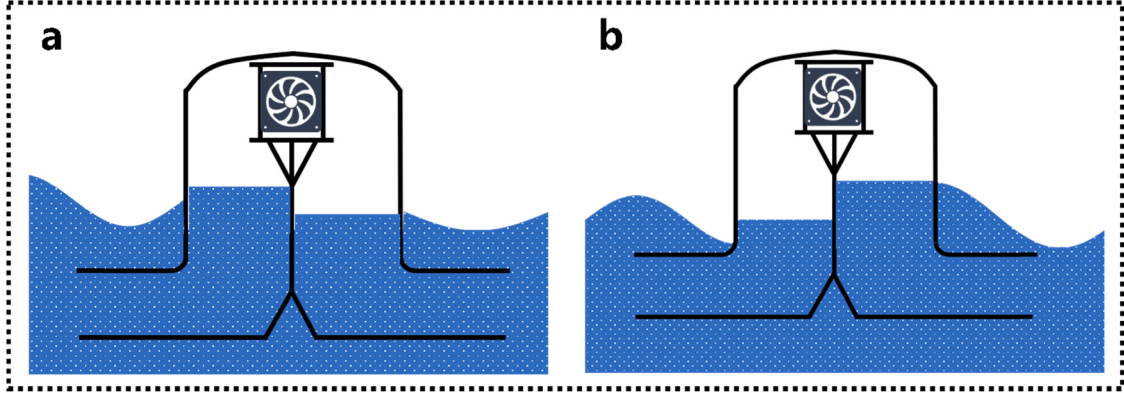
Fig. 7. Double chambered backward bent duct buoy (BBDB)
(adapted from [114]).
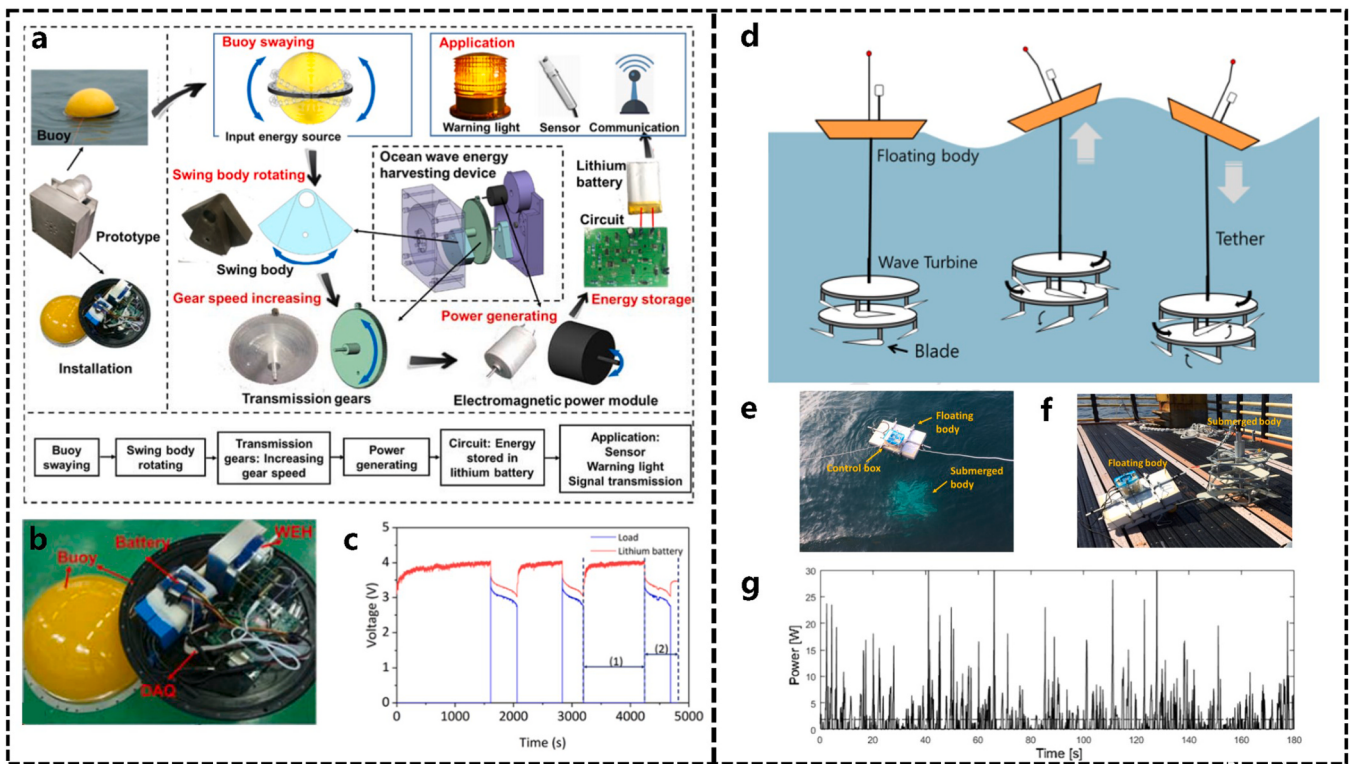
**Fig. 8.** (a) Architecture of the OKEH system. (b) In-ocean test: The installation of OKEH. (c) Voltage across the battery and load in the power management circuit during the charging and discharging process. (d) Operation principle, sea trial, and (e), (f) hardware configuration of the mooring-less sensor buoy. (g) Time series of hydrodynamic power during the sea-trial in 3 min.
(a–c) Reproduced with permission from CC BY-ND 4.0 [102]. (d–g) Reproduced with permission from Elsevier [96].

ultra-low frequency waves and drive the high-speed rotating electromagnetic rotor through the gear. The power management circuit enables it to charge and discharge the lithium battery automatically. Fig. 8 (b) shows the OKEH installed in a real-sea test. In Fig. 8 (c), the OKEH includes three working cycles and can realize the function of a continuous power supply. When the wave height is greater than 0.6 m, the maximum peak-to-peak output voltage is 15.9 V, the corresponding power is 0.13 W, and the maximum power density is 31 W/m^3 [102]. The authors claim that it can power various low-power sensors and promises the effective improvement of the life of marine buoys [102].

2.2.4. Wave induction turbine mode

To reduce the deployment and maintenance costs, Joe et al. proposed a design to power a mooring-less sensor buoy [96]. As shown in Fig. 8

(d), the design is based on a submerged body and a floating body. The submerged body is a self-adjusting wave induction turbine and utilizes the heave motion of waves to drive the rotor. The rotor has flap-type blades and rotates as the waves rise and fall. It is unaffected by the waves coming from various directions and does not require mooring. By adjusting the rope, the submerged body is located at the wave base (that is, the depth at the wave excitation force becomes negligible, usually 5 m below the sea surface). In an ocean, the mooring-less sensor buoy can continuously convert wave energy into electric energy, and reduces the installation costs and improves the battery life. Fig. 8 (e–g) shows the test performed in real seas under medium sea states. The average turbine speed is 11.20 rpm, the average power is 1.61 W, and the maximum power is 37.68 W [96]. The author suggests that the power can be further improved based on a more suitable energy management in the

later stage [96].

2.3. Electroactive polymers harvester

For distributed sensors in the ocean, reliable and sustainable power is essential [107]. EAH plays an important role in utilizing OKE for generating electricity [108–123]. Generally, according to the material classification, there are mainly three types of EAHs; based on dielectric elastomer (DE) material, piezoelectric material, and ionic polymer metal composite (IPMC) material [113]. In the following sections, the application of EAHs in OKE collection for powering distributed ocean sensors is introduced.

2.3.1. Dielectric elastomer

Dielectric elastomer harvesters (DEHs) have a high flexibility and a large elongation ability and can adopt to various materials [108]. Therefore, the DEH has been conveniently utilized as sensors, actuators, or energy harvesters in the past few years [108–114]. In addition, creating a low-cost energy harvester is gaining a lot of attention [108]. Fig. 9 depicts the basic working mechanism of DEHs. In Fig. 9, the DEH is regarded as a variable capacitance device in the generator mode. When an external force excites the DEH, it stretches from form (I) to form (II) with no charge present on the electrodes. At position (III), a charge Q is deposited on the electrodes; this is called "priming" [124]. In the next step, the charge on the electrodes is assumed to be constant, and the external force contracts the film (IV) (low capacitance) and resists the electrostatic forces, causing an increase in the electrostatic energy stored in the DEH. Finally, in stage (IV), the DEH gets fully discharged, and the stored electrostatic energy is recovered [124].

The output of DEH depends on the capacitance variation in a single cycle. If the area variation during a cycle is known, the output can be determined as follows:

$$E = \gamma \varepsilon \varepsilon_0 v_0 E^2_{max} \ln\left[\frac{A_i}{A_f}\right] \tag{3}$$

Here, γ is the efficiency of energy conversion, ε is the dielectric constant of the dielectric elastomer material, and ε_0 is the permittivity of free space; v_0 is the volume of the constant film; E_{max} is the maximum electric field across the polymer; A_i and A_f are the total capacitances of the dielectric elastomer layers in the stretched and unstretched states, respectively.

Prahlad et al. found that DE materials have a satisfactory impedance matching with the waves [108]. The exclusive characteristic of the DEH

is that, instead of requiring a large centralized wave generator, it only requires a local power supply in the ocean. A cable-anchored DE material may be used to generate electricity. Although the electricity produced by DE is relatively small, it is sufficient to power ocean sensors [108].

Kim et al. studied a pseudo-OWC-type DEH, as displayed in Fig. 10 (a) [113]. The basic structure is a simple tubular column that is immersed in water and anchored to the sea floor. The DE membrane (gray) is fixed on the top of the column. As the wave passes through the cylinder, the pressure difference is changed between the upper and lower column, causing the DE film to deform. For a device with a diameter of 2 m and containing 787 DE films with a thickness of 31.25 μm, the authors predict that, under the condition of a wave height of 3 m and a period of 10 s, the total energy of each incident wave can reach 6.18 kJ and the power can reach 0.618 kW [113].

Although the exploit of small-scale prototypes for harvesting wave energy has been demonstrated, utilizing electroactive polymers to obtain flow energy remains an enormous challenge [111]. Based on the simplified design concept and environmentally friendly development, Maas et al. developed a flowing energy converter (FEC) [111]. In Fig. 10 (b), the elastic tube with a DE material is covered with waterproof electrodes on its surfaces. There is a rigid ring at the end, to stretch and contract the FEC. The active valve is initially opened and is controlled by an external mechanical structure. As shown in Fig. 10 b(i), the flow forces the rigid ring and subsequently, the tube is pre-stretched to a certain extent. As shown in Fig. 10 b(ii), the active valve closes the outlet of the tube watertight. Due to the sudden closure, the water pressure increases significantly and the elastic DE material stretches in the direction of flow, and the kinetic energy is converted into strain energy. At the maximum stretch, the FEC has to be charged, as shown in Fig. 9. Because of the reflected wave at the open inlet of the tube, a negative pressure occurs inside the tube, and the tube contracts below its initial length (Fig. 10 b(iii)). At the minimum length, the FEC is discharged and the active valve opens the tube (Fig. 10 (iv)). Finally, the DE stretches to its initial length (Fig. 10 b(v)) and the mechanical cycle starts again. For a FEC device with an inner diameter of 65 mm, a thickness of 2.5 mm, and a length of 1 m, it can close the pinch valve within 100 ms, and a shock wave travels through the inner tube at a speed of approximately 2.5 ms⁻¹ [111]. As an energy harvesting system, the device has the advantages of scalability, resource efficiency, and lightweightedness [111]. However, it is limited by the design and layout of the active valve.
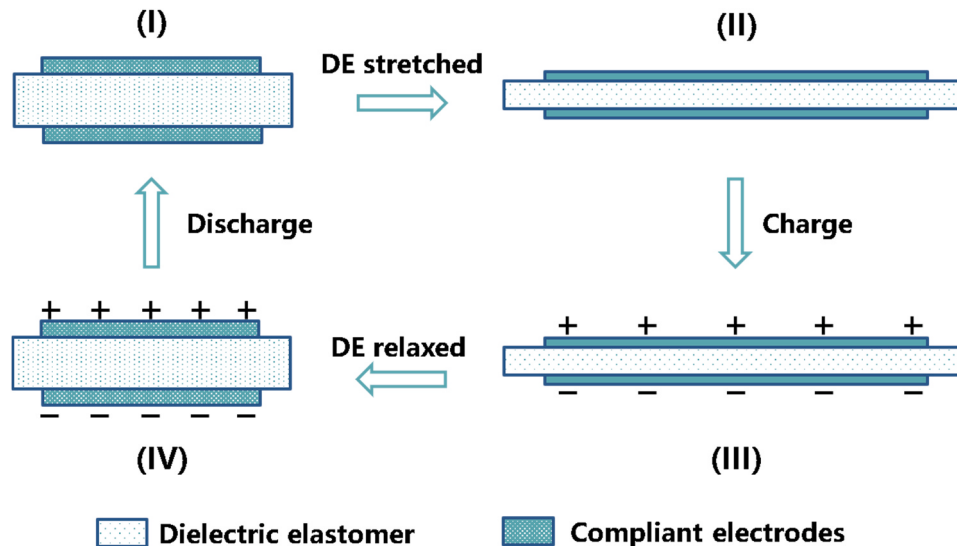

**Fig. 9.** Generating mechanism of DEH.
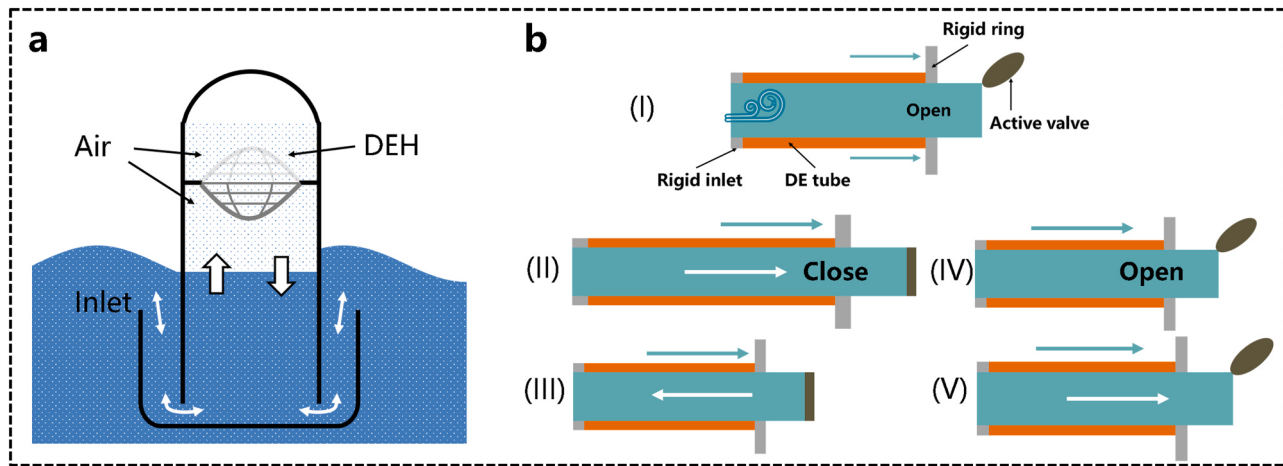
Fig. 10. (a) Pseudo-OWC-type DEH. (b) Mechanical design and working principle of the flow energy converter in the opened and closed state.

2.3.2. Piezoelectric harvester

Due to the unique ability to couple electrical signals and mechanical displacements, the sensor and actuator technologies commonly adopt piezoelectric materials to change the electrical polarization in response to mechanical stress or to produce mechanical strain in response to an electric field [125–131]. The commonly used piezoelectric materials are the piezoelectric ceramic transducer (PZT) and polyvinylidene fluoride (PVDF) [132]. Specifically, PZT, also known as lead zirconate titanate, is a poled ferroelectric ceramic with a perovskite structure [132] and PVDF is a poled electroactive polymer with its piezoelectric response approximately 10 times higher than that of the other polymers [133].

The piezoelectric harvester (PEH) is composed of a piezoelectric element coupled with a mechanical structure. Fig. 11 (a) presents a typical piezoelectric generator. A mass m_a is attached to the tip of a cantilever beam. When subject to waves, the cantilever beam oscillates and generates bending stress along the beam. Thereafter, the mechanical deformation polarizes the piezoelectric element in the direction of the thickness and produces voltage signals between the electrodes. Typically, a PEH can be modeled as a rigid mass coupled with a damper, spring, and piezoelectric structure that operates around its resonance frequency and undergoes linear movement [134,135], as shown in Fig. 11 (b) [136]. The rigid body is coupled to the fixed surface through springs, dampers, and piezoelectric elements. Assuming that the applied force is harmonic, the model of the PEH can be expressed as [132].

$$F = j\omega m v + b v + \frac{S}{j\omega} v + F_i. \qquad (4)$$

Here, the harmonic term $e^{j\omega t}$ has been suppressed [136], while m and v are the mass and velocity of the rigid mass, respectively. F_i is the amplitude of the internal mutual force between the piezoelectric element and the rigid mass, s is the spring stiffness, and b is the damper

coefficient. The circuit equivalent model facilitates the determination of the relationship between the device output and frequency, elastic modulus, and device structural parameters.

Few PEHs have been proposed to collect energy from wind and vortex-induced vibration [132, 137–143]. Recently, various applications of piezoelectric materials have been observed in the field of OKE harvesting.

Taylor et al. developed an energy harvesting eel (Eel) to convert the kinetic energy into electricity for powering remote sensors and robots [137]. The Eel utilizes a slender strip of PVDF piezoelectric polymer that swims in the current, emulating an eel in water. In non-turbulent flow, the front bluff body of the Eel will periodically emit alternating vortex on both sides. The eddy current forces the slender trips and produces pressure difference and allows the Eel deformation under forced oscillation to generate an AC voltage. Each strip covers three layers, namely a central inactive layer (core) and two active layers of piezoelectric material, bonded to each side of the central layer. Each system contains five Eels. The length, width, and thickness of the Eels are 132 cm × 15.24 cm × 400 μm. In a flow of 1 m/s, the Eel can provide the output of 1 W, and the energy conversion efficiency is approximately 33%. Such Eels are capable of charging the batteries or capacitors of distributed robot groups or remote sensor arrays, thereby extending the mission life of the ocean containing flowing water indefinitely [137].

Mutsuda et al. designed a flexible wave energy harvester, named flexible piezoelectric device (FPED) [144]. Fig. 12 (a) demonstrate the FPED consisting of a thin PVDF laminated layer and an elastic material coated with a piezoelectric layer. The piezoelectric material is directly coated on the substrates and electrodes using a spray nozzle device. The elastic material is highly durable and can withstand extreme bending and weathering caused by the ocean waves and currents. Fig. 12 (b) displays the output of a FPED with the dimensions of 200 mm
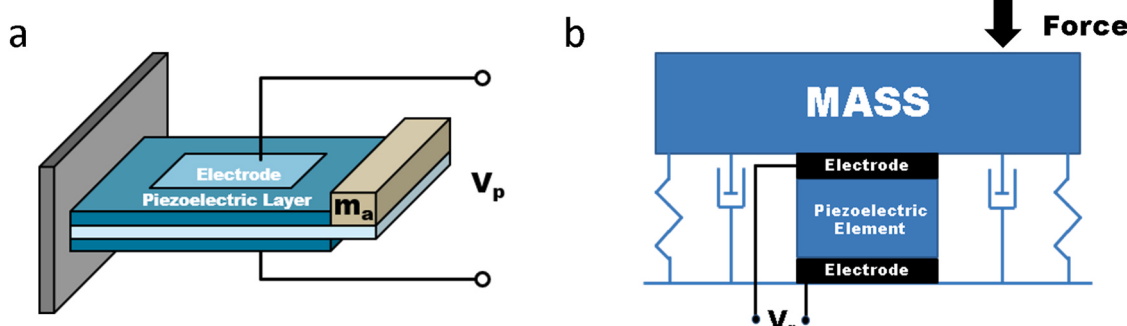

Fig. 11. Piezoelectric harvester model. (a) Cantilever beam (common piezoelectric-based power generator). (b) Modeling of a piezoelectric power generator.
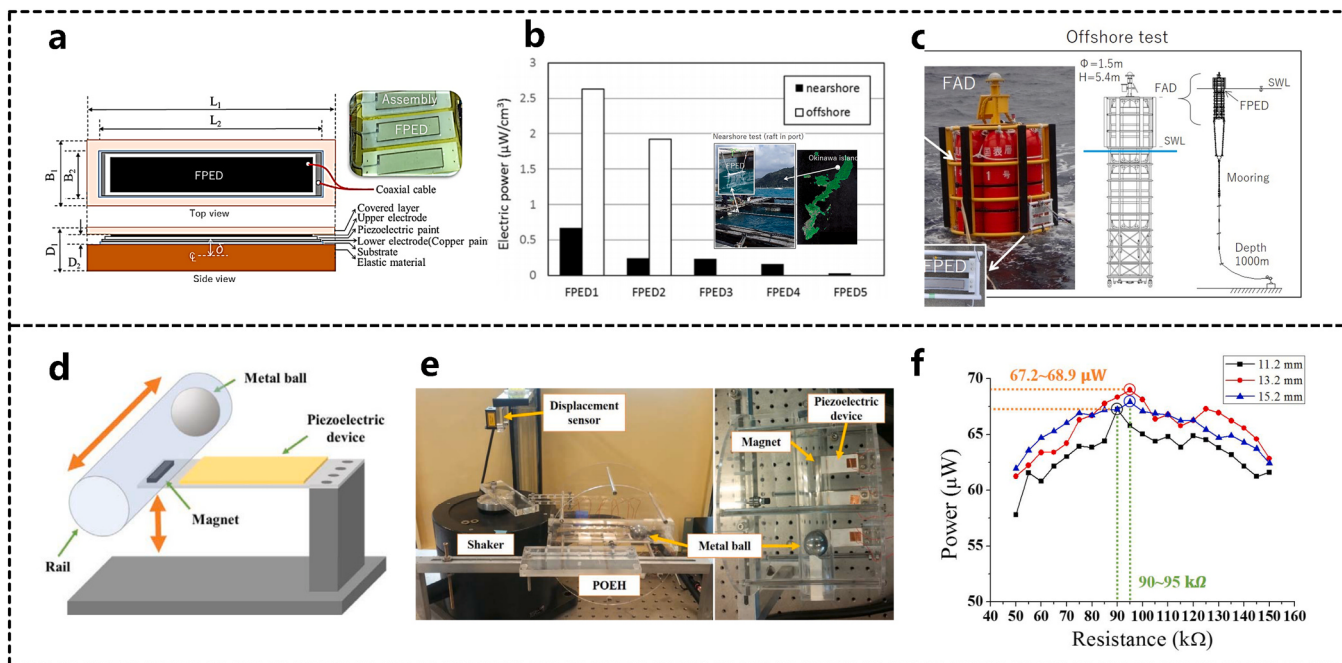
Fig. 12. (a) Laminated structure of a FPED painted by spray nozzle. (b) Comparison of electric power generated from each FPED at nearshore and (c) offshore sites. (d) PEH based on sway movement. (e) Test bench construction. (f) Output power of the device for three different shaker displacement values. (a–c) Reproduced with permission from Elsevier [144]. (d–f) Reproduced with permission from Elsevier [145].

(length) × 60 mm (width) × 5 mm (thickness) for a test conducted nearshore and offshore. The power density of the FPED can reach 2.6 μW/cm³. Based on the FPED, Mutsuda et al. further proposed elastic floating unit with hanging structures (EFHAS) with a suspension structure [146]. The EFHAS includes a floating unit and suspension unit. The suspension unit is connected by six FPEDs, covering three horizontal FPEDs and three vertical FPEDs. The vertical FPEDs can collect current energy and vortex energy, while the horizontal FPEDs can collect wave energy. Compared with the previous harvesters, the unique advantage of EHFAS is that it can collect OKE. The author states that the EFHAS can not only produce electricity, but also utilize the energy for wireless sensing, including environmental monitoring, mechanical sensing, and structural diagnosis (such as, protecting offshore wind turbines from ocean waves) [146]. When used in an artificial marine infrastructure, the electricity generated by the EFHAS can be used to direct fish to feeding areas, while ensuring their safety, thereby contributing to the establishment of an environmentally friendly ecosystem [144, 146–148].

Hwang et al. reported a PEH based on sway motion, as shown in Fig. 12 (d). It mainly consists of a piezoelectric cantilever structure and a magnet [145]. A catheter with a metal ball is placed above the magnet and works at the tip of the piezoelectric module. Fig. 12 (e) is a schematic diagram of the test bench, and the system is tested based on a setting that simulates ocean waves. In Fig. 12 (f), for a device with the dimensions of 3.8 cm × 1.9 cm × 0.2 cm at a simulated wave frequency of 0.5 Hz, the maximum output voltage is 21.1 V, and the power density is 47.85 μW/m³ [145]. The authors believe that they can adapt the "multi-directional vibration" approach to develop PEHs that can be operated at low frequencies and applied in "sea-based" applications involving buoys and boats [145].

In addition, Murray et al. designed a two-stage energy harvester with two decoupling systems [149]. It is used in a buoyant environment to convert the unstable low-frequency movement into a constant high-frequency mechanical vibration. The low-frequency movement of the primary system will excite the several piezoelectric vibration elements (secondary systems). Accordingly, the heaving buoy continuously transforms the low-frequency wave vibration into the resonance of the vibratory piezoelectric element array. The conversion efficiency of the two-stage energy harvester can reach 33% under the resonance condition. The expected output of a 76 mm diameter, 910 mm long spar buoy is 60–180 mW [149]. The novel design could replace batteries or other finite-storage technologies to power the small, remote, and unmoored buoys [149].

2.3.3. Ionic polymer metal composite harvesters

Piezoelectric materials have demonstrated amazing power generation performances in several applications. However, their fragility and the characteristic of only responding to high-frequency stimuli have limited their further application. IPMC is an excellent candidate for harvesting energy in the low frequency regime due to its inherent flexibility, long life, and mechanoelectrical coupling [117]. So far, most of the research concentrated on the signal conditioning circuit, and energy harvesting has not received adequate attention [117, 122, 150–153].

In Fig. 13 (a), Kim et al. displayed the world's first OKEH based on an IPMC material [113]. This is the first research to use IPMC materials to power marine monitoring equipment or marine platforms [113]. It is composed of multiple Nafion films coated with graphene-based inks. In this study, the novel developed graphene-based IPMC has been tested in ocean. As shown in Fig. 13 (b), the device can supply electricity to distributed ocean monitoring equipment or stand-alone offshore plants with a target of 120–600 Wh over 20 d [112]. Although it is estimated that the output is weak in the ocean and the growth of algae/barnacles on the module will retard the bending motion of the IPMC and disrupt the collection of electrical energy, the module is inexpensive and durable and can be modified to adapt to different types of applications [113].

2.4. Triboelectric nanogenerator

The large-scale electromagnetic generator is currently the main technology for wave energy collection. However, due to the low efficiency of the EMG under irregular and low-frequency (< 5 Hz) ocean waves, the equipment manufacturing and maintenance costs are extremely high [70, 74, 154–162]. Recently, researchers are
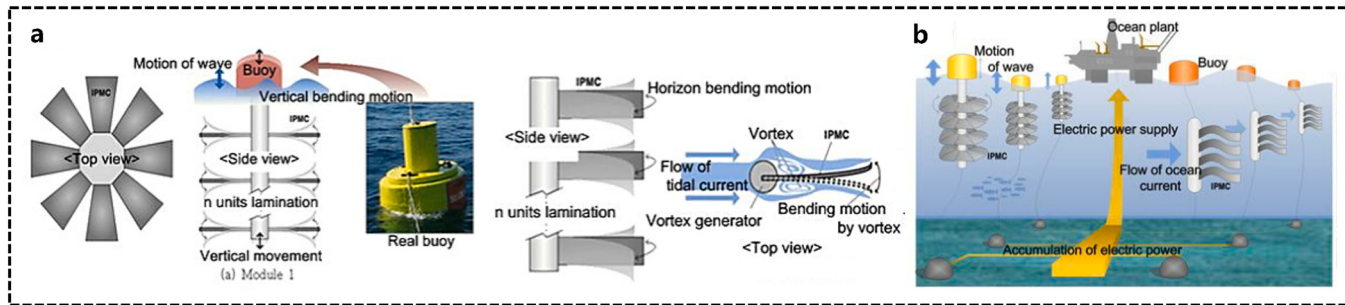
Fig. 13. (a) Illustration of a compact movable power system utilizing both vertical wave and horizontal ocean current with a vortex, and (b) schematics of the OKE harvesting structure with the IPMC supplying electricity for stand-alone offshore plants.
(a,b) Reproduced with permission from Springer [113].

increasingly inclined to develop novel harvesters that are low-cost, long-lived, environmentally friendly, and corrosion resistant [70, 163–178,180]. Remarkably, Professor Wang found that collecting electrical energy from mechanical friction is an effective and inexpensive approach and accordingly, the TENG was proposed [100,155, 182–190]. The subsequent studies have confirmed that TENG can obtain electric power from "disordered" energy in various environments, such as wave energy, human motion, and vibration energy in the surrounding [191–198]. TENG has obvious advantages over the EMG in the energy collection of low-frequency waves with a frequency lower than 5 Hz [70, 74]. In addition, the feedback mechanism between the mechanical vibration and the output suggests that TENG can promote energy utilization in the IoT era [87,199]. Therefore, researches has proposed the construction of TENG as an effective approach for blue energy harvesting and marine environment monitoring [70,156,158,164,189,200, 201].

2.4.1. The four fundamental working modes

The basic TENG physical model bases on the Maxwell's displacement current and can be defined as [88]:

$$J_D = \frac{\partial D}{\partial t} = \varepsilon \frac{\partial E}{\partial t} + \frac{\partial P_s}{\partial t} \tag{5}$$

Where D is the displacement field, ε is the dielectric constant of the

medium, E is the electric field, and P_S is the polarization created by the piezoelectric or triboelectric effect [68,87,155,202]. The first term on the right hand refers to the electric field that changes with time and is related to the origin of electromagnetic. The second term comes from surface polarization and is the basics of nanogenerators [88,203,204].

As shown in Fig. 14 (a), the contact-separation TENG works based on the polarization in vertical direction. Physical contact between two dielectric films (dielectric layer 1 and 2, and at least one of them is an insulator) with distinct electron affinities creates oppositely charged surfaces. When the two layers are separated by a gap, a potential drop is created between the two electrodes. The free electrons in electrode 1 or 2 would flow to the other electrode through external circuit and balance the electrostatic field. Once the gap is closed, a potential drop is created by the triboelectric charges will disappear and the induced electrons will flow back. Thus, a periodic contact and separation between the two dielectrics can cause AC output in the external circuit. The corresponding equation is:

$$V = -\frac{Q}{S\varepsilon_0}[d_0 + x(t)] + \frac{\sigma x(t)}{\varepsilon_0} \tag{6}$$

Here, σ is the static charge density, S is the metal area, ε_0 is the permittivity of free space, d_0 is the effective dielectric thickness and $x_{(t)}$ is the time dependent distance between the two tribo-material [205].

The lateral sliding mode TENG uses the polarization in lateral di-
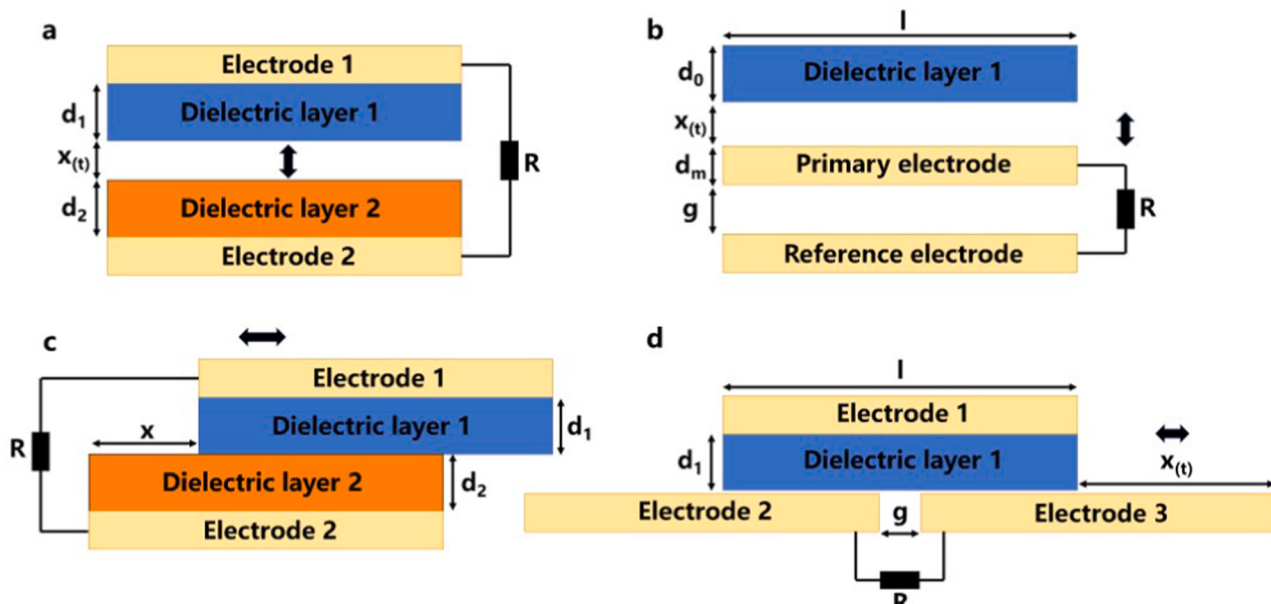
Fig. 14. The working principle of TENG: (a) Basic vertical contact-separation working mode, (b) lateral sliding working mode, (c) single-electrode working mode and (d) freestanding working mode of TENGs.

rection caused by the relative sliding between two dielectrics [205]. Once two materials with opposite triboelectric polarities get contact, surface charge will transferred due to the triboelectrification effect (Fig. 14 (b)). If the two surfaces are fully matched, no current flow will take place since the positive charges at one side are fully compensated by the negative ones. Once a relative displacement is introduced by an externally applied force in the direction parallel to the interface, triboelectric charges will not be fully compensated at the displaced/mismatched areas and create an effective polarization. In other words, a tribo-polarization occurs along the sliding direction by a change in the effective contact area [205]. Therefore, a potential difference is generated across the two electrodes. The sliding mode can be made fully packaged and even in rotation mode so that it can operate in vacuum. The output voltage of the lateral sliding mode TENG can be calculated by the following formula with w being the transversal width:

$$V = -\frac{d_0}{w\varepsilon_0(1-x)}Q + \frac{\sigma d_0 x}{\varepsilon_0(1-x)} \qquad (7)$$

The single electrode mode TENG is better to harvest energy from a freely moving object without attaching conduction lines. As shown in Fig. 14 (c), if a charged dielectric approaches the metal plate, an induction current will be generated on the metal plate to balance the field. Once the dielectric moves away from the metal plate, the current flows back to the ground. Such mode of TENG is most useful for utilizing the energy from a moving object. The theoretical electrical outputs can be expressed:

$$Q_{sc} = \frac{\sigma wl}{1+\frac{C_1(x)}{C_2(x)}} \qquad (8)$$

$$V_{oc} = \frac{\sigma wl C_2}{C_1 C_2 + C_2 C_3 + C_1 C_3} \qquad (9)$$

In the above equations, l is the length in the longitudinal direction, C_i is the equivalent capacitance formed between electrical nodes [205].

The freestanding mode TENG, with its working mechanism displayed in Fig. 14 (d), can effectively store charges and is suitable for wave energy harvesting. When the two active dielectric layers get contact, triboelectric charges will be induced on the surface. Eq. (10) expresses the voltage of the general freestanding TENG, where g is the gap between the reference and the primary electrodes.

$$V = \frac{d_0 + g}{\varepsilon_0 s}Q + \frac{2\sigma x}{\varepsilon_0} \qquad (10)$$

Notably, when a charge induced by friction, electrodes 2 and 3 do not need to contact the top dielectric layer directly. Therefore, in the rotating mode, the power generation unit (electrodes 2 and 3) can rotate freely without direct mechanical contact, which extends the service life of TENG.

2.4.2. Rolling-structure mode

Previous researches suggest that TENG provides a lightweight, cost-effective approach for converting various vibration energy into electricity [155,163,164,178,186,190,206–217]. Nowadays, wave energy harvesting based on TENG has become a research hotspot, which is expected to become the technical foundation for the in-situ power supply of ocean sensors.

Wang et al. opened the TENG in wave energy harvesting and proposes a rolling-structured freestanding triboelectric-layer-based nanogenerator named RF-TENG (Fig. 15 (a)) [154]. The RF-TENG contains a rolling ball (Nylon) and a Kapton (Polyethylene-Naphtholate) film coated on the internal spherical shell. It works based on the contact electrification effect between traditional polymer materials, with the advantages of light weight, low cost, and exceptional charge transfer efficiency under low frequency. The structural optimization results show that a spherical TENG with 6.0 cm diameter can provide a peak current

of 1 μA and an instantaneous output power of up to 10 mW. As shown in Fig. 15 (b) and (c), the TENG can directly drive tens of LEDs and charge a series of supercapacitors to a rated voltage within several hours at the wave frequency of 1.43 Hz. Thus, the authors believe that RF-TENG, with its self-powered support system is an effective green energy technology [154].

On top of this, Fig. 15 (d), Zhang et al. proposed a sea snake structured triboelectric nanogenerator (SS-TENG) [187]. The SS-TENG works in the freestanding-layer mode. When excited by waves, the internal PTFE balls roll back and forth between the electrodes, generating AC across the external resistance. The SS-TENG has the characteristics of light weight, simple structure and low cost, and it can effectively harvest energy from low amplitude ocean waves [187]. Fig. 15 (e) shows the maximum power of the SS-TENG can reach about 4 μW. Although the researchers have claimed that the SS-TENG could be used in actual ocean conditions with high salinity, the electrical energy collected by this device had not meet the power requirements of ocean wireless sensor network. Nevertheless, it is interesting to note that when more SS-TENG units are connected in parallel, the output voltage will increase exponentially, which provides a feasible method for improving the output performance of TENGs, as demonstrated in Fig. 15 (f).

By designing a tower-like triboelectric nanogenerator (T-TENG), Xu et al. [156]. significantly enhance the output of TENG-based OKEH. As plotted in Fig. 15 (g), the T-TENG is composed of multiple parallel TENG units. Each unit covers several PTFE balls, a metal electrode membrane and a 3D printed arc surface coated with a melt adhesive reticulation nylon film (Fig. 15 (h)). The experimental results suggest that the T-TENG can effectively convert arbitrary directional and low-frequency wave energy into electrical energy by utilizing charged PTFE balls to roll on an arc surface. It is further noted that the power density of the T-TENG increases proportionally with the number of units connected in parallel without rectifiers due to its distinctive mechanism and structure (Fig. 15 (i)) [156]. Finally, a maximum power density reaches 11 W/m³ with 10 TENG units connected. Therefore, the design of T-TENG is considered as an innovative and effective approach for large-scale blue energy harvesting by connecting more blocks to form T-TENG networks [156].

In Fig. 15 (j), Cheng et al. reported a soft spherical triboelectric nanogenerator (SS-TENG) to increase the output of spherical TENG [207]. It uses acrylic hollow spheres as the shell and a rolling flexible liquid/silicone as the soft core. Due to the significant increase in contact area, the maximum transferred charge (Q_{sc}) with a diameter of 3.9 cm can reach about 500 nC, as displayed in Fig. 15 (k). Compared with the traditional spherical TENG, it adopts soft core to replace inertial hard ball, and the output performance is improved by 10 times [207]. By reasonably controlling the softness of the power generation element, the output of SS-TENG can be adjusted to match the frequency of the external wave. Fig. 15 (l) shows it can charge a 2.2 μF capacitor to approximately 3 V in 40 s at the wave frequency of 2 Hz [207].

In addition, an breakthrough in generator network performance was achieved by Yang et al. [183]. The research group developed a self-assembled wave energy harvesting network based on high-performance TENGs. For a single spherical TENG with a package diameter of 8 cm, the average power density under wave excitation is 8.69 W/m³, 18 times more than the average power of the shell structured TENG [183]. In terms of the self-assembled networking, the rotatable nested magnetic ball structure is used to realize the magnetic connection between TENG units. As indicated by the authors, the self-assembled network may pave the way for the application of large-scale triboelectric nanogenerator networks for powering ocean sensors [183].

2.4.3. Liquid-solid mode

The above-mentioned TENGs studies are based on the direct contact of two solid materials with different electronegativity. In order to reduce the influence of seawater corrosion and electrostatic interference on
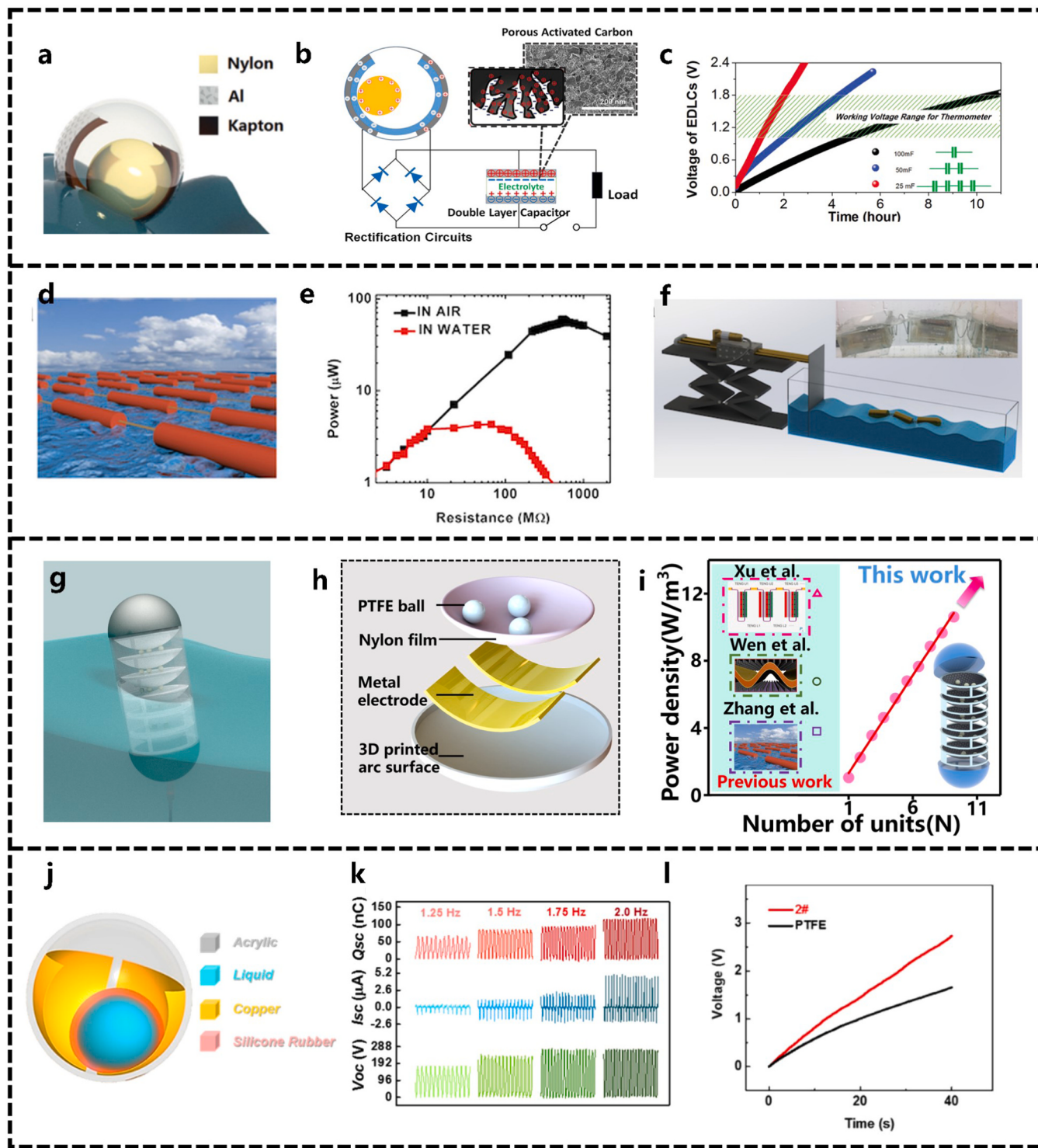
Fig. 15. RF-TENG, (a) The freestanding-structured design of RF-TENG. (b) Schematic diagrams of the self-power system with TENG, rectification circuits, EDLC, and load. (c) The charging curves for one, two, and four EDLC capacitors in series, respectively. SS-TENG. (d) Array of sea snake triboelectric nanogenerators on an ocean energy farm. (e) Voltage vs time of SS-TENG without air gap in the water at different concentrations of NaCl. (f) The placement of the SS-TENG in the water environment with a linear motor actuating the water waves. T-TENG. (g) Schematic diagram of the designed tower-like TENG consisting of multiple units. (h) The internal structure of one unit and the nylon film coated on the 3D printed arc surface. (i) Comparison of the power density of the present T-TENG and previous TENGs. (j) Structural scheme of the soft-contact model spherical TENG (SS-TENG) with a flexible rolling sphere. (k) Typical electric output curves of SS-TENG under various working frequencies. (l) The charging curves of SS-TENG and S-TENG for a capacitor (2.2 µF) at the frequency of 2 Hz.
(a–c) Reproduced with permission from Wiley [154]. (d–f) Reproduced with permission from Elsevier [187]. (g–i) Reproduced with permission from American Chemical Society [156]. (g–l) Reproduced with permission from Elsevier [207].

TENG, Li et al. fabricated a liquid–solid triboelectric nanogenerator (LS-TENG) [200]. Fig. 16 (a) and (b) shows the physical structure and application scenario of LS-TENG. Compared with the solid–solid TENG with the same contact area, the output has been magnified by 48.7 times. The output voltage, current and transfer charge of the LS-TENGs network can reach 290 µA, 300 V and 16,725 nC, respectively. This suggests that the LS-TENGs network can directly power hundreds of LEDs and drive a radio frequency emitter to form a self-powered wireless save our souls (SOS) system in marine emergency. Moreover, the buoy-like LS-TENG can harvest energy from different types of low-frequency vibration, including up–down, shaking and rotation movements. Thus, the authors concluded that this work rendered an innovative and effective approach toward large-scale blue energy harvesting and applications [200].

Liu et al. designed a special cable TENG with its integral and internal structure, as shown in Fig. 16 (c) [218]. It consists of two spring steel strips and three polymer films. The spring steel strip inside the cable is of high elasticity and good fatigue resistance, and is suitable for long-term operation. The wires sandwiched between the two spring steel strips are protected from seawater corrosion. The contact-separation movement can produce considerable electrical energy output. The most significant advantage of this structure is that spring steel and other materials are used as the rigid connection structure between the cable TENG units. Experimental analysis shows that a single TENG cable can achieve a maximum voltage of 36 V and a maximum transfer charge of 26 nC in one cycle. Finally, in Fig. 16 (d), the multiple connected TENG cables are tested in a water tank, and the output voltage of the four TENG cables does not drop significantly after rectification. Thus, the novel design can prevent the entanglement between the units, protect the transmission line from seawater erosion or interference and eliminate the ionization in the seawater [218].

2.4.4. Disk and rotation mode

In Fig. 17 (a), Jiang et al. reported a TENG with a robust swing-structure for ultra-low frequency wave energy harvesting (SS-TENG) [219]. Its characteristic is that the air gap inside the device and the flexible brush can realize the smallest friction resistance and sustainable friction charge, thereby enhancing the robustness and durability. The SS-TENG with dimensions of 7 cm and 7.5 m s^{-2} has a maximum output of 342 V, 5.9 µA and 256 nC. The maximum and average power density can reach 144.3 mW/m^3 and 26.3 mW/m^3, respectively. The theoretical energy conversion efficiency is 28.2%, and the electrical output performance remains unchanged after 4,000,000 cycles of continuous triggering [219]. Fig. 17 (b) shows that the SS-TENG successfully power
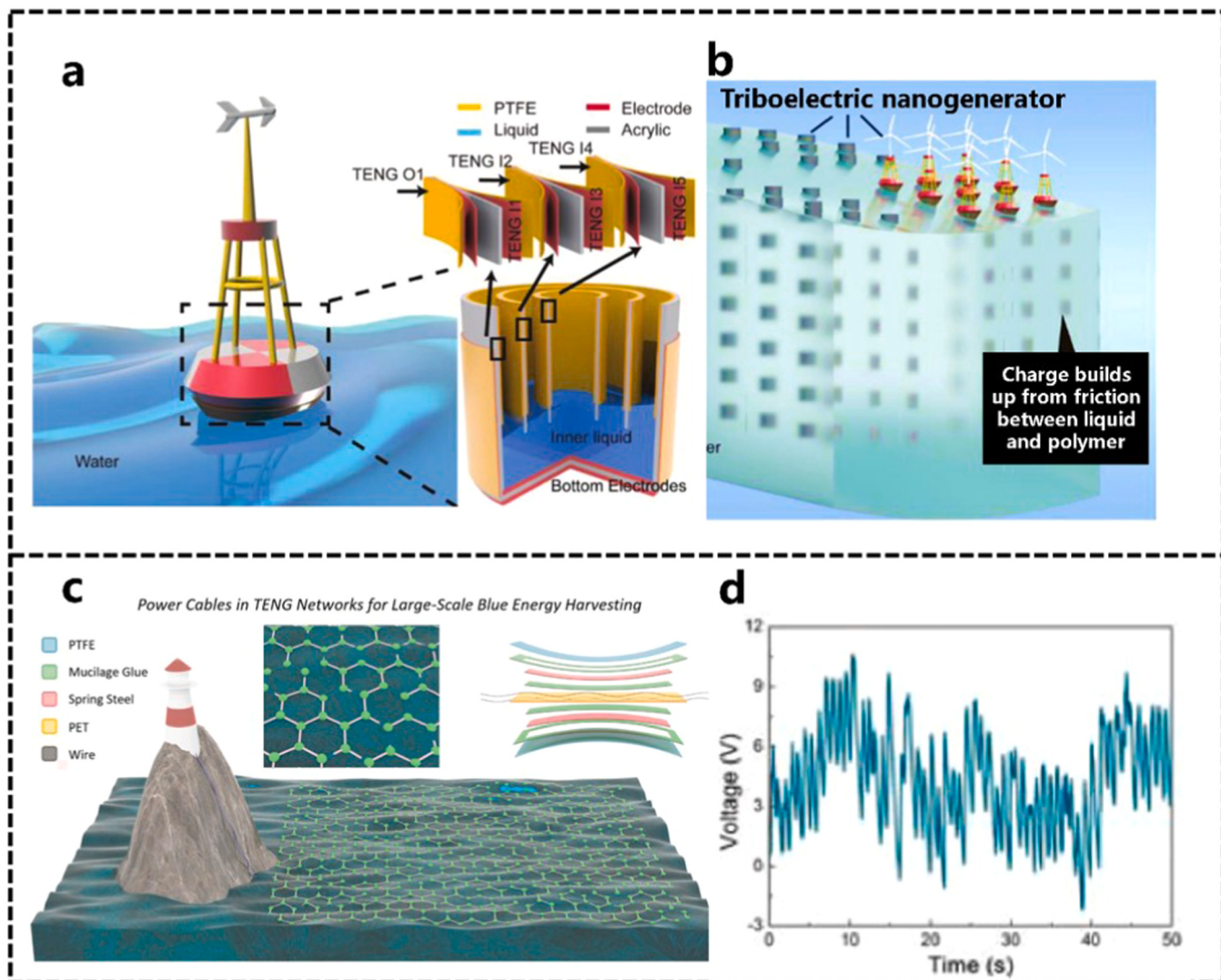
**Fig. 16.** (a) The structure of liquid–solid-contact buoy triboelectric nanogenerators. (b) The schematic illustration of the TENG network which contains thousands of single units. (c) TENGs connected by power cables for large-scale blue energy harvesting with honeycomb-like topology structure. (d) Output voltage of four cables. (a,b) Reproduced with permission from Wiley [200]. (c,d) Reproduced with permission from Elsevier [218].
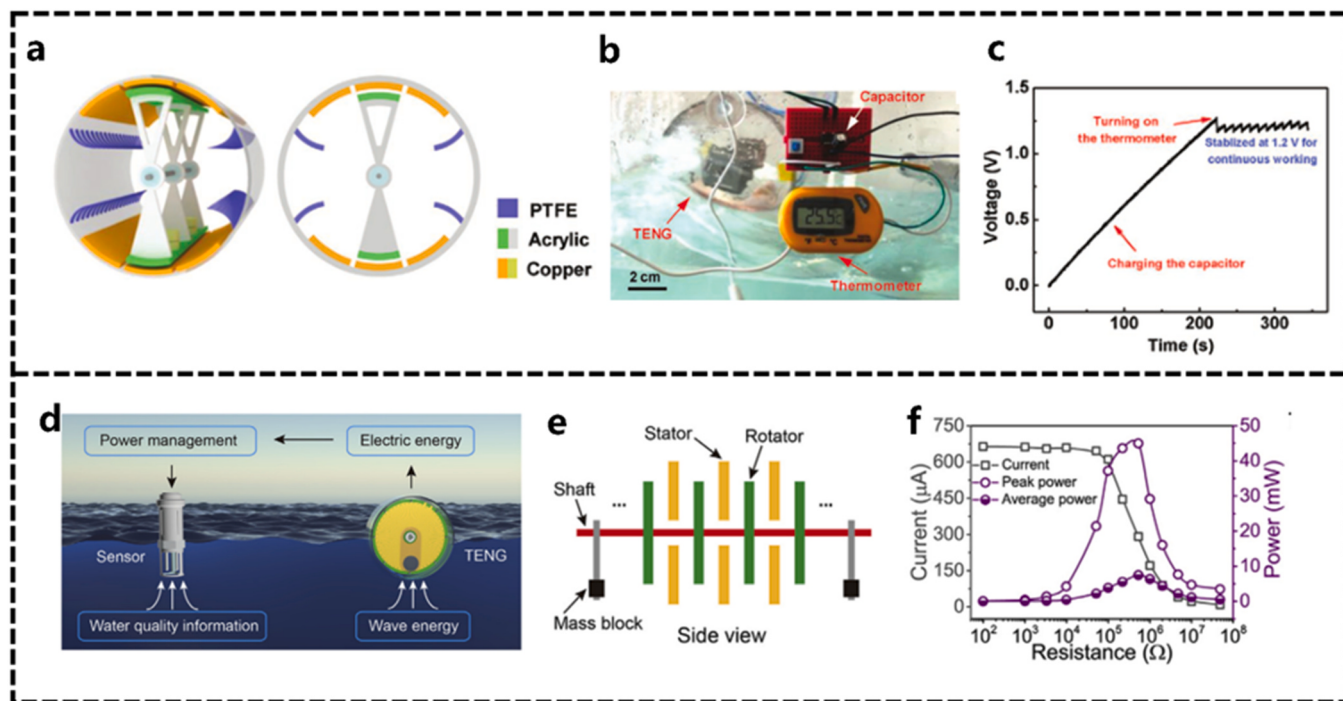
Fig. 17. (a) Schematic diagram of the 3D structure and cross-section for the SS-TENG. (b) Photograph of a digital thermometer powered by the SS-TENG and (c) the charging process for a capacitor of 220 μF to power the thermometer under the wave conditions of 10 cm and 1.2 Hz. (d) Schematic diagram of the water quality monitoring system and the illustration of the side view (e) of the TD-TENG. (f) The peak current, peak power and average power of the TD-TENG under various loads in water.
(a–c) Reproduced with permission from Wiley [219]. (d–f) Reproduced with permission from Elsevier [158].
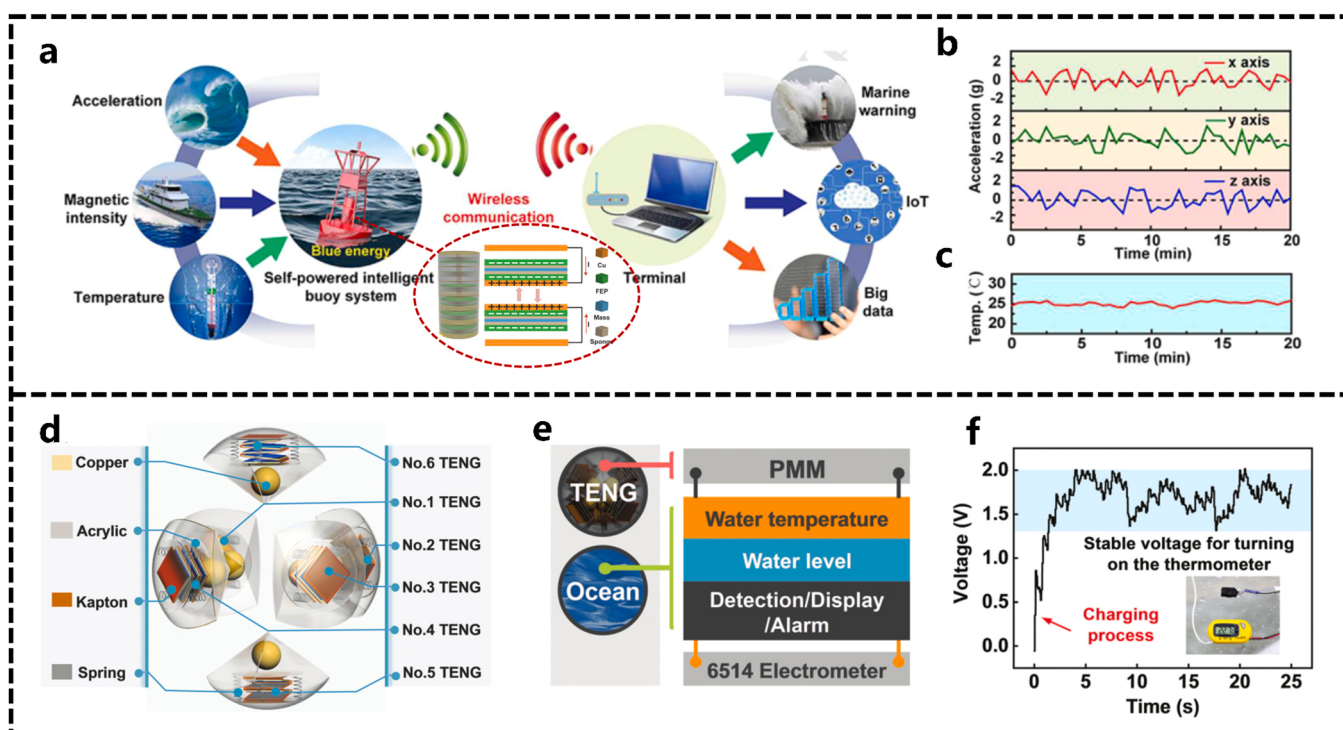
Fig. 18. The SIBS for sustainable and autonomous wireless sensing (a) and data transmission driven by wave energy (b), (c). (d) Exploded view of the spherical TENG. (e) Framework for the integrated marine information detection/display/alarm system driven by the power-managed spherical TENG. (f) Application demonstration for powering a digital thermometer.
(a,b) Reproduced with permission from Elsevier [220]. (c,d) Reproduced with permission from Royal Society of Chemistry [221].

a portable electronic product under waves. In Fig. 17 (c). The thermometer is successfully powered for self-powered sensing and environment monitoring, which proves its potential application in self-powered temperature sensing and blue energy environmental monitoring [219].

In order to enable ocean sensors to continuously and stably monitor water quality, a new energy harvester is urgently needed for monitoring equipment [158]. To this end, Bai et al. designed a high-performance

tandem disk triboelectric nanogenerator (TD-TENG) to collect wave energy (Fig. 17 (d)) [158]. Fig. 17 (e) displays that it adopts a radial grating disc structure to convert the agitation of low-frequency waves into high-frequency electric energy. The friction surface is made of frosted material, which greatly improves the rotation of the TENG rotor disc in water. In this way, the peak and average power of the TENG reached 45.0 mW and 7.5 mW, respectively, as show in Fig. 17 (f) [158]. Besides, through a convenient power management circuit, the
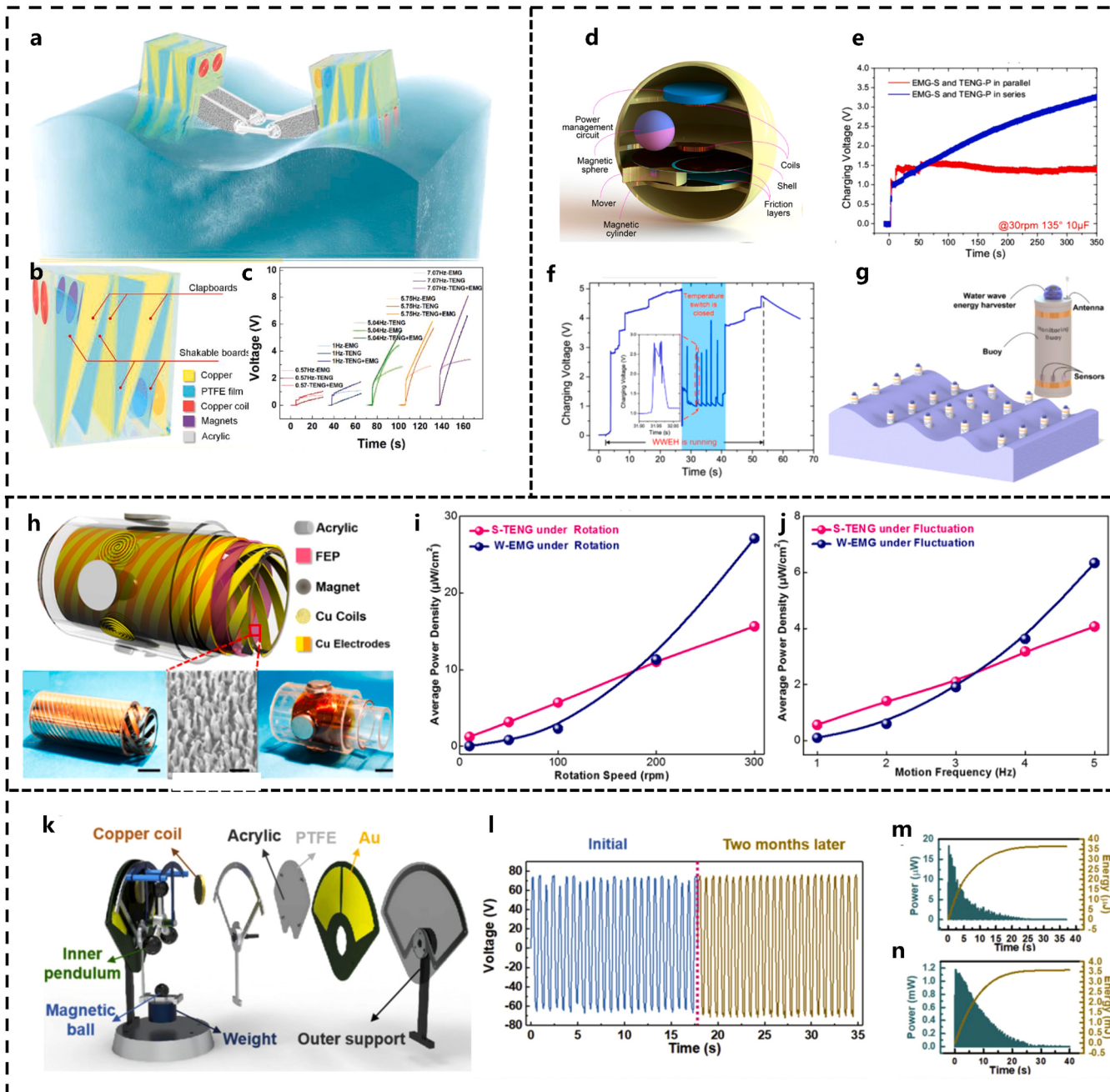
Fig. 19. Structural design of ocean energy hybrid nanogenerator. (a) Schematic illustration of the hybrid system with a double-wing structure riding on the water wave, which is basically constituted by (b) a cubic structured unit hybridizing TENG and EMG. (c) Charging performances of TENG, EMG, and hybrid nanogenerator for a capacitor of 10 μF at different water wave frequencies. (d) Schematic diagram of the WWEH and (e) charging characteristics of the TENG-P and EMG-S connected in parallel and in series. (f) Typical working waveform of the temperature alarm system. (g) Schematic illustration of the buoy network based on the WWEH for environmental monitoring. (h) Structure design of the blue energy hybrid nanogenerator [222]. The optimized average power densities of S-TENG and W-EMG under (i) rotation and (j) fluctuation modes. (k) Structural schematic diagram of the HH based on inertia pendulum. (l) Stability of the triboelectric nanogenerator. Output power and converted energy of TENG (m) and EMG (n) for a trigger with impedance of 400 MΩ.
(a–c) Reproduced with permission from Wiley [184]. (d–g) Reproduced with permission from American Chemical Society [223]. (h–j) Reproduced with permission from American Chemical Society[222]. (k–n) Reproduced with permission from Elsevier [224].

short-circuit current increases to 11 mA, and can fully meet the power supply for water quality monitoring equipment. It creates a way to solve the power bottleneck of the multifunctional sensing platform that needs to work autonomously in water [158].

2.4.5. Contact-separation mode

Xi et al. designed a self-powered intelligent buoy system (SIBS) by using a multilayered-TENG for harvesting wave energy, as displayed in Fig. 18 (a) [220]. The TENG unit operates in the contact-separation mode and can yield an average output power density of 13.2 mW/m^2 with the wave frequency of 2 Hz. In Fig. 18 (b) and (c), the SIBS can achieve a sustainable and autonomous wireless sensing of vibration acceleration, magnetic intensity and temperature within a range of 15 m. A power management module is adopted in the micro program control unit (MCU) to form an intelligent monitoring mechanism, so that the collected energy can be allocated to sensors with different priorities [220]. Thus, the authors believe that SIBS can provide a universal platform for powering ocean sensors and has broad prospects in the internet of things, big data, artificial intelligence and blue energy [220].

Based on a spring-assisted multilayered structure, Liang et al. manufactured a spherical TENG to collect multi-directional wave energy (Fig. 18 (d)) [221]. It can achieve a maximum output of 80 μA, 250 V and 8.5 mW under the wave frequency of 1.0 Hz. Fig. 18 (e) shows integrating a power management module (PMM) to manage the output energy of the TENG. Through integration with PMM, a stable and continuous DC voltage can be generated on the load resistance, as shown in Fig. 18 (f). Once a 0.1 F supercapacitor is charged, the stored energy is increased by 100 times. Further, the TENG device is used to power the digital thermometer and the water level detection/alarm device successfully, which proves its broad application prospects for powering ocean sensors [221].

2.5. Hybrid harvesters

The development of marine technology requires energy harvesters to collect blue energy efficiently under different sea states. Multiple studies have shown that the integration of various energy harvesting technologies (namely hybrid harvesters, HHs) seems to be a very promising solution [70, 223, 225–227].

Wang et al. proposed a hybrid wave energy harvester based on TENG and EMH (Fig. 19 (a)) [184]. As demonstrated in Fig. 19 (b), the TENG consists of an acrylic box and four shakable boards pasted with flexible PTFE films. The acrylic box is divided into four separate chambers and Cu electrodes are anchored on the internal walls of each chamber. The PTFE film is attached on the board to get full contact with Cu electrodes under wave excitation [184]. In this wok, the contact-freestanding mode is first utilized to enhance the efficiency of energy harvesting [184]. The charging characteristics of TENG, EMG and the hybrid nanogenerator are obtained by using a 10 μF capacitor at different wave frequencies, and their charging curves are plotted in Fig. 19 (c). For TENG, it can get a V_{oc} of 400 V and a maximum I_{sc} of 15.3 μA from the simulated water wave, while the EMG obtained a V_{oc} of 1.7 V and an I_{sc} of 5.4 mA. The integration of TENG and EMG achieves compensation of their respective advantages, enabling the hybrid system to provide satisfactory output in a wide range of operating frequencies (0.2–7 Hz) [184].

Wu et al. presented a HH based on water wave energy harvester (WWEH), as shown in Fig. 19 (d) [223]. The electrodes of the WWEH design as the Tai Chi shape in order to achieve an ideally performance. Two coils are adopted to transform the motion of the magnetic sphere into electricity. The charging curves of the device in Fig. 19 (e) illustrates that the series connection of EMG-S (i.e. two coils connected in series) and TENG-P (i.e. two friction layers connected in parallel) are undoubtedly the best scheme [223]. Moreover, the WWEH adapts a paper-based supercapacitor for power management circuit to power temperature alarm system, as illustrated in Fig. 19 (f). The performance of the WWEH is tested in Lake Lanier on a buoy. The results indicate the

supercapacitor can be charged to 1.84 V and the electric energy storage can reach about 1.64 mJ within 162 s [223]. This work demonstrates the WWEH can be successfully utilized to drive distributed ocean sensors for environmental monitoring.

As shown in Fig. 19 (h), Wen et al. reported a HH consists of a spiral-interdigitated-electrode triboelectric nanogenerator (S-TENG) and a wrap-around electromagnetic generator (W-EMG) for harvesting OKE [222]. Notably, due to the unique structural design, the HH could collect energy in ocean tide, current, and wave energy to generate electricity under either rotation mode or translation mode [222]. The Fig. 19 (i) and (j) shows that the S-TENG is irreplaceable for harvesting energy with low rotation speeds (< 100 rpm) or low motion frequencies (< 2 Hz), while the W-EMG is able to produce larger output at high frequencies (> 10 Hz). Thus, the complementary output can be maximized and the hybridized nanogenerator can harvest energy in a broader frequency range. The proposed hybrid nanogenerator renders an effective and sustainable progress in practical applications of the hybrid nanogenerator toward harvesting water wave energy offered by nature [222].

Chen et al. proposed a disordered pendulum type HH integrated with a power management circuit to power ocean sensors through wave energy, as shown in Fig. 19 (k) [224]. The maximum output power of TENG can reach 15.21 μW, and the EMG can reach 1.23 mW, and can light up about 100 LEDs [224]. Moreover, this work has realized the long-distance wireless transmission of sensors signals, and the data transmission capacity can exceed 300 m. Fig. 19 (i)–(n) shows it has excellent long life and stable output performance. The author believes that this can become a new direction for collecting low-frequency vibration energy from the marine environment, aerospace and industry [224].

Fig. 20 (a) shows a concept based on point absorber type wave energy harvester operating with both EMG and TENG. Due to the wave excitations, the slider in linear motor oscillates up and down to generate electricity. In Fig. 20 (b), the rectified outputs of the EMG phases are connected in series and then connected to the rectified TEMG [228]. This kind of connection can maximize the output. As shown in Fig. 20 (c), the hybrid system displays a great boost not only in the magnitude, but also in the speed of charging voltage. In terms of output, a maximum I_{sc} of 59 μA at 3 Hz is obtained and the power density reaches 271.1 W/m^{-3}(TENG) and 700 W/m^{-3} [205]. As illustrated in Fig. 20 (d), Lee et al. designed a blue hybrid energy harvester based on a friction-electromagnetic hybrid generator [230]. Fig. 20 (e) and (f) shows by using a newly designed hybrid circuit, the output power can reach 95.4 mW under a 100 Ω load, and an IoT platform has been established to monitor humidity and temperature around the clock [230].

Furthermore, Feng et al. designed a HH that uses the flexible rabbit fur as an electric brush [229]. The brush has the function of pumping charge onto the dielectric surface, thus reducing the operating resistance and improving the durability of the device. At a frequency of 0.1 Hz, the peak power density is 10.16 W/m^3 and the average power density is 0.23 W/m^3 [229]. This HH has successfully realized self-powered temperature mapping and wireless transmission. Liang et al. developed a new type of charge excitation circuit (CEC) specially for HH, which has greatly improved the output performance [227]. A maximum power density of 49.3 W/m^3 and an enhanced current of 25.1 mA have been reached [227]. The device can monitor the marine environment by transmitting radio frequency (RF) signals and it can also power wireless communication systems successfully [227].

3. Comparison and prospects

3.1. Comparisons among all technologies

3.1.1. Comparison of OKEHs

It is worth noting that the goal is to utilize the various "disordered"
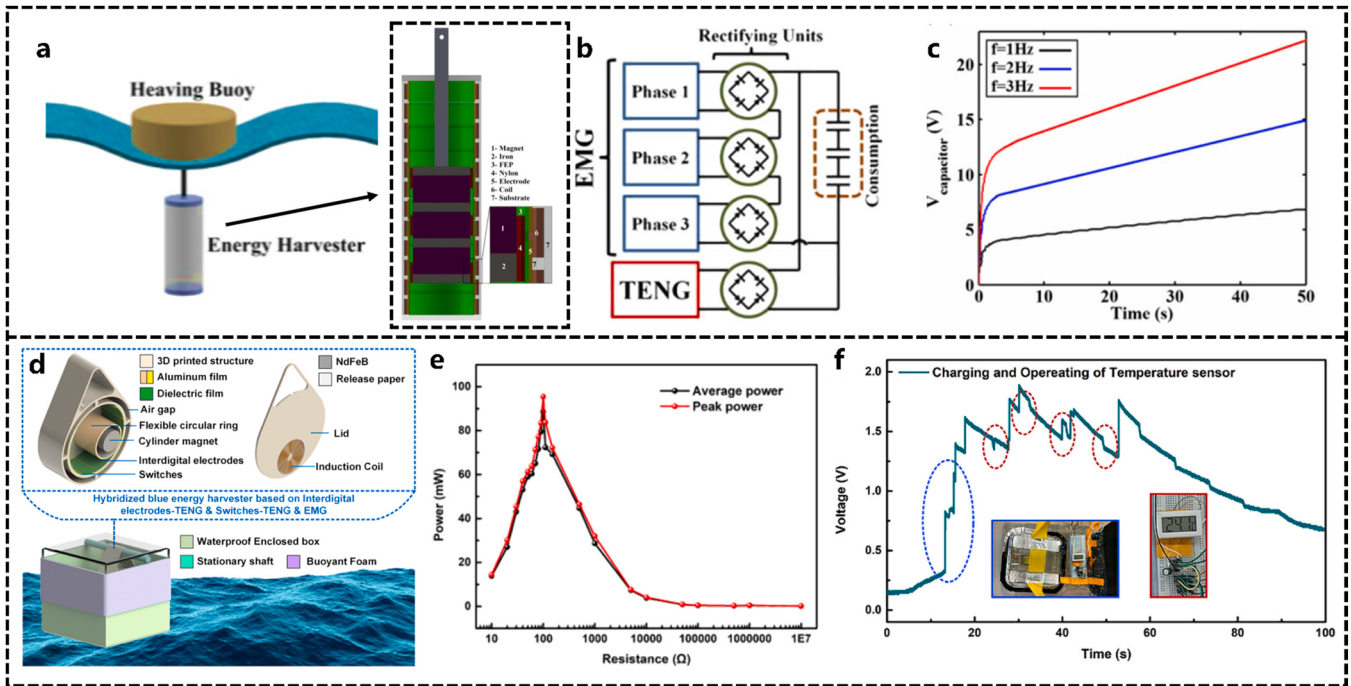
Fig. 20. (a) Schematic and the internal structure of the HH floating on waves surface. The (b) Schematic configuration and (c) capacitor charging curves for different motion frequencies of the hybridized system. (d) Schematic diagram of the pendulum structure containing an Interdigital electrodes-TENG (I-TENG), a Switches-TENG (S-TENG) and an Electromagnetic generator (EMG). (e) Output power under different load resistance. (f) Voltage curve as a temperature sensor is powered with the hybridized blue energy harvester and working continuously.
(a–c) Reproduced with permission from Wiley [228]. (d–f) Reproduced with permission from Elsevier [230].

forms of kinetic energy in the ocean to supply power for numerous distributed ocean sensors, rather than building large-scale centralized OKEHs [100,108]. In recent years, EMH, EAH, and TENG have made progress in small-scale OKE for powering distributed sensors. Four approaches for collecting OKE, EMHs, EAHs, TENGs, and HHs, have been reviewed in this article and their respective energy conversion performances and characteristics are summarized in Fig. 21.

For the EMH, the Lorentz force induces the electrons to flow in a conductor. The EAH produces electricity mainly based on the fluid-induced vibration and the coupling between the generation parts and mechanical motion. TENG functions based on the principles of tribo-electrification and electrostatic induction. The future scope for the further study on TENG to harvest current energy is enormous. Although TENG is studied extensively for wave energy conversion, these studies have not considered the mooring systems or wind/wave loads. The current applications are limited to shallow water or small waves in deep water. Compared with wave energy, energy is more abundant in tidal currents nearshore and also generous in the ocean currents offshore. With ocean currents, it has the advantages of high predictability, low flow rate, stable energy, and wide distribution. To realize the self-supply of ocean sensors, TENG, as a low-cost and high-entropy energy harvester, can be deployed not only on ocean surfaces, but also underwater.

In Fig. 21, TENG, EAH, HH and most small-scale EMHs have their own advantages in flow-mechanical-electric conversion due to their simple structure and less-complicated internal mechanical structure. Among them, TENG is a favorable approach for harvesting low-frequency, low-amplitude, and random-direction wave energy (called high entropy energy). First, it is an exceptional choice as the power source for micro-nano systems that may be crucial for the ocean IoT sensor networks [87]. Second, because the voltage of TENG is high and is less related to the running frequency, TENG can be matched with various commercial sensors in the market. Third, the cost of TENG is low, the structure is simple, and the damage of a single unit will not

affect the overall performance. A hybridization of TENG with the other harvesters is recommended for a general case. However, due to the lack of universal metrics, comparing the different technologies has proved to be a complex task [162]. To evaluate the level of OKEHs to power distributed ocean sensors, five key properties has been set as the criteria that include the output voltage, output current, power density, cost-effectiveness, and robustness. The corresponding radar charts are presented in Fig. 21. Robustness is a measure of the ability of a subsystem or device to experience a survival event outside the expected design conditions, and not sustain damage or loss of functionality beyond an acceptable level, allowing a return to an acceptable level of operation after the event have passed [233]. In the case of the partial destruction of an OKEH, the smaller final destruction degree indicates a stronger robustness. Currently, collecting scientific evidence to quantitatively evaluate the robustness and cost-effectiveness of each transduction mechanism is still complicated. To resolve this problem, the method proposed by Mariello et al. is adopted in this review [162]. After a comprehensive study of the existing literature, a dynamic picture representing the current OKEH development status has been obtained that can be used to evaluate the pros and cons of each technology. As shown in Fig. 21, the pentagon covering the largest surface represents the most suitable energy harvester for distributed monitoring equipment and sensors in the ocean. Specifically, the HH appears to be the ideal harvester to power ocean sensors at present. HH combines the advantages of EMH and TENG. TENG can provide the highest voltage, while EMH can provide the highest current. The advantage of EAH lies in its satisfactory robustness. Due to its unique material and flexible structure, it can maintain stability even under extreme sea states. However, the lower voltage and current make it only capable of powering a small number of ocean sensors. In the following parts, the five characteristics of the radar chart are summarized into three aspects: materials, output, and application scenarios. Both the choice of materials and application scenarios are the indicators of cost-effectiveness, and the robustness is a comprehensive result of the various causes in the system.
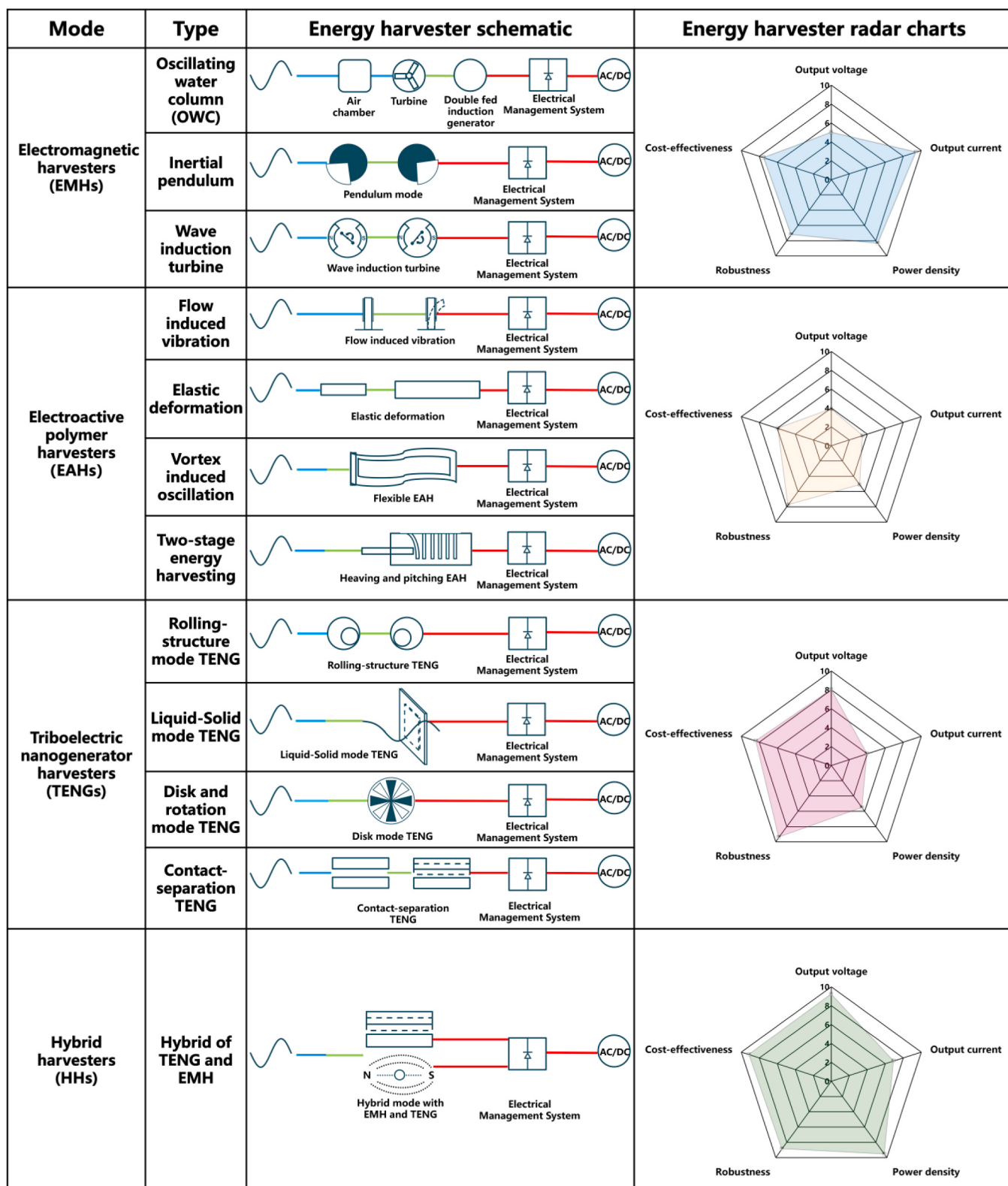
Fig. 21. Flow-machine-electrical conversion and the characteristics of the various OKEHs: OWC [103], inertial pendulum [102,105], wave induction turbine [96], flow induced vibration [112,113,144,146,231], dielectric elastomer [111,113], vortex induced oscillation [137], two-stage energy harvesting [232], rolling-structure mode TENG [154,156,187,207], liquid-solid mode TENG [200,218], disk mode TENG [158,219], contact-separation TENG [220,221], and hybrid TENG [183,184, 223,224].

3.1.2. Comparison of output

The method proposed by Mariello et al. is selected for the power density calculation [162]:

$$P = \frac{P_{out}}{V}, \tag{11}$$

where P_{out} is the instantaneous peak electrical power output, and V is the volume of the device. It is calculated that the highest instantaneous peak power density of EMHs, EAHs, TENGs, and HHs are 553 W/m^3, 43 W/m^3, 60.93 W/m^3, and 971.1 W/m^3, respectively. The detailed comparison is shown in Table 1. The research of EAH mainly focuses on numerical simulation and lab testing. In addition, most EAHs can only fulfill few small marine sensors for environmental monitoring, mechanical sensing, and structural diagnosis. Furthermore, the TENGs and HHs have been tested in real seas and can provide power for small marine monitoring equipment and sensors. They are usually characterized by a high mobility, environmental adaptability, and anti-interference ability for powering distributed ocean sensors. Therefore, with the further research of TENG, it is expected to match various types

of commercial sensors or larger marine monitoring equipment, such as, AUV, ROV, and Glider, to provide a foundation for smart ocean.

3.1.3. Comparison of materials

In terms of the EMH, the selection of power generation materials includes the rotor and stator. Currently, most rotor materials are permanent magnets (such as, NdFeB) [234], while the stator is mainly made of rigid materials to reduce magnetic resistance. The distinguished feature of the PEH is the application of piezoelectric anticorrosive materials, such as, PVDF, PZT, and tourmaline, that makes it possible to cope with the extremely harsh sea conditions and seawater erosion. The TENG can adopt much inexpensive dielectric friction materials, such as, PTFE, Nylon, FEP, aluminum, and copper, that significantly reduce the cost and threshold of generators [143, 191–193, 195–198, 229, 235–238]. In addition, the solid-solid contact, liquid-solid contact, or suspension induction methods can be utilized between the TENG power generation components to avoid damage (such as, excessive piezoelectric device variables) and improve the stability and endurance of the ocean sensors.

Table 1
Comparison of OKEH in terms of the type, materials, power source, output, and applications.

Mode	Type	Representative harvester	Major material	Power source	Power density	Applications
Electromagnetic harvesters (EMH)	OWC	BBDB [103]	Permanent magnet	Wave	11.3 W/m^3; 78% (Theoretically)	Ideal design for powering marine ranches and sensor node
	Inertial pendulum	Ding et al. [105]	Permanent magnet	Wave	N/A	Ideal design for powering the sensors in underwater glider or platforms
		OWEH [102]	Permanent magnet		31 W/m^3 (Instantaneous output power, real sea test)	Powering sensors and improving buoy service life
	Wave induction turbine	Mooring-less sensor buoy [96]	Permanent magnet	Wave	553 W/m^3 (Real sea test)	Powering sensor buoy
Electroactive polymers harvesters (EAH)	Flow induced vibration	EFED, EFHAS [144,146]	PVDF; Silicon; PDMS	Wave	0.6–2.9 μW/cm^3 (Real sea test)	Powering buoy
		IMPC [112,113, 115,117]	Nafion film; Graphene-based inks	Current and Wave	N/A	
	Dielectric elastomer	Pseudo-OWC [113]	DE material	Wave	N/A	Ideal design for powering distributed ocean sensors (prospect)
		FEC [111]		Current	N/A	
	Vortex induced oscillation	Eel [137]	PVDF	Current	N/A	Ideal design for powering remote sensors and robots (prospect)
	Two-stage energy harvesting	Two-stage [232]	PZT; PVDF	Wave	14.4–43 W/m^3; 33% (Theoretical experiment)	Ideal design for powering the small, remote, and unmoored buoys
Triboelectric nanogenerator harvesters (TENG)	Rolling-structure mode TENG	RF-TENG [154] SS-TENG [187] T-TENG [156] SS-TENG [207]	Nylon; Kapton; Aluminum; Silicone	Wave	8 W/m^3–11 W/m^3 (Sink test)	Powering buoy, temperature sensor, super capacitor, and LEDs
	Liquid-Solid mode TENG	LS-TENG [200] Cable TENG [218]	PTFE; Copper; PDMS	Wave	60.93 W/m^3 (Sink test) N/A (Sink test)	Power buoy, wireless SOS system wireless sensor, cable, and LEDs
	Disk and rotation mode TENG	SS-TENG [219] TD-TENG [158]	Epoxy glass fiber; Copper; PTFE; Acrylic	Wave	144.3 mW/m^3 (Sink test) 7.3 W/m^3 (Sink and real sea test)	Power buoy, water quality sensors, wireless transmitter, and thermometer
	Contact-separation TENG	SIBS [220] Liang et al. [221]	Copper, FEP, Kapton, PTFE, Acrylic, sponge	Wave	13.2 mW/m^2; (Sink test) 36.83 W/m^3 under 1.0 Hz (Real sea test)	Power marine information detection/display/alarm system, buoy, wireless sensor, digital thermometer, and LEDs
Hybrid harvesters (HH)	Hybrid TENG	Wang et al. [184]	Permanent magnets; PTFE; Copper Coil	Wave	10.2 W/m^3 (TENG) + 15.3 W/m^3 (EMH) (Sink test)	Powering buoy, wireless sensing node system, digital thermometer, and LEDs
		WWEH [223]		Wave	N/A (Real sea test)	
		Wen et al. [222]		Wave, tidal, ocean current	N/A (Sink test)	
		Chen et al. [224].		Wave	0.82 W/m^3 (TENG) + 66.6 W/m^3 (EMH) (Real sea test)	
		Saadatnia et al. [228]		Wave	271.1 W/m^3 (TENG) + 700 W/m^3 (EMH) (Sink test)	
		Lee et al. [230]		Wave	94 W/m^3 (Hybrid) (Sink test)	

3.1.4. Comparison of application scenarios

With respect to the application scenarios, different OKEHs correspond to various marine monitoring equipment or sensors. Because the current ocean monitoring nodes are heterogeneous, highly-distributed, and mobile, it is necessary to understand the power supply. Apparently, except for the AUV, ROV, and sonar equipped with numerous ocean sensors, OKEH can completely meet the power demand of marine sensors with energy requirements below 20 W. The ocean sensors can be characterized by wide distribution, low power consumption, high precision, robust sensing, mobility, heterogeneity, and high reliability. These also introduce higher requirements for the existing OKEHs. The hybrid TENG has shown its advantages in ocean sensing and made remarkable progress. The subsequent OKEH design should have efficient resource utilization to reduce the cost of manufacturing, deployment, operation, and maintenance. On this basis, a hybrid energy harvesting system can utilize the several renewable power sources comprehensively, such as, solar, tidal, and wind energy that is suggested for marine environment monitoring in the future.

3.2. Prospects

This study systematically reviews the four OKEHs currently used to power ocean sensors through analyzing the energy conversion, materials, output, and application fields. The OKEHs for powering distributed ocean sensors in the marine environment is still in its early stage and has a long way ahead. In view of the demand for the small-scale energy utilization of distributed ocean sensors, the following recommendations are proposed for the future design of OKEH.

3.2.1. Enhancement of OKEH output

The usage of proper materials can improve the effectiveness and output efficiency of OKEHs in many marine applications. For material selection, while ensuring the excellent power generation performance of OKEH, environmentally friendly and anti-corrosion materials should be appropriately selected to reduce microplastics in the ocean.

The design of OKEHs should ensure sufficient flexibility and can be customized to adapt to heterogeneous ocean sensors. It is critical to minimize the number of connectors because they are sensitive to marine corrosion. The OKEHs should utilize novel resources to reduce the manufacturing, deployment, operation, and maintenance costs. It should be easy to maintain and disassemble, that includes replacing the power supply system, replacing or calibrating the sensors used, and recycling after completing the monitoring tasks.

At sea, the ocean monitors or sensors are usually integrated into a sensor node, such as, a buoy or an underwater vehicle, as shown in Fig. 1 and 2. With respect to the OKEH, using a single collection method can provide a small amount of energy continuously; however, it cannot provide high power in a short time. Different types of sensors have different energy requirements due to the heterogeneous characteristics. It can lead to load fluctuations and may force the specifications to exceed the requirements while designing OKEH. Therefore, for small-scale OKE acquisition, the OKEHs based on two/multiple-stage hybrid power may be more practical.

3.2.2. Highly efficient power management system

Energy storage technologies affect the size, cost, and operating life of the node [31]. Therefore, effective power management is extremely essential to maximize the energy. Nowadays, while using energy harvesters in ocean sensors, the common metrics (such as, remaining battery power) are no longer available for power management [3]. Instead, the best decision must be made about the future availability of energy. To this end, an algorithm can be developed to adaptively learn the environment around ocean sensors and to efficiently use energy to improve the performance of the sensor network. In addition, a power management system can be developed to study the transfer process from OKE to stored electrical energy. Owing to the optimization of the design

of energy harvester and power transmission, the efficiency of conversion and transferring electrical energy to the ocean sensors is improving. By incorporating power management with these schemes, a large amount of energy can be conserved, resulting in decreased issues related to harvesting.

3.2.3. Integration of energy harvester, power management circuit, energy storage, and sensor system

Growing marine unmanned systems and sensors are rapidly promoting the innovation of marine monitoring. The evolution of ocean sensor not only miniaturizes marine unmanned systems, but also leads to its widespread utilization. It enables a wide application in in-situ energy harvesting by combining ocean energy harvesting techniques. The OKEH described in this review is adopted as an energy storage device to power sensors or monitoring equipment. According to the working principles of EMHs, EAHs, TENG, and HHs, it is expected to realize the in-situ power supply and self-powering in marine monitoring. By integrating the energy harvesting function into the system of ocean sensors, it is possible to achieve a coverage of the ocean sensor network for reasonable observation/monitoring, governance, and further exploration. An envisaged ocean sensor node generally consists of the following three main modules:

(1) An ocean sensing module for data acquisition and incorporates several probes and sensors (Fig. 22).
(2) A wireless transceiver module for wireless data communication and consists of a radio frequency (RF) transceiver and an antenna to send data and receive instructions from the sink node [17].

(3) A power supply module usually consisting of energy storage equipment (rechargeable batteries), power management systems, and energy harvesters (OKEH, solar energy harvesters, wind energy harvesters, and thermal energy harvesters).

In the early working state, an analysis of the available energy sources from ocean should be performed to convert the irregular, high-entropy energy into regular electrical energy. To exploit these orderly energies, one or more energy sources must be selected and composed into the power management system to obtain the effective electrical energy. For durability and hybrid topologies, an energy storage technology should be added to the system to ensure the long-term and stable operation of ocean sensors. The next stage is to use the energy supply module to power the ocean sensing module and the wireless transceiver module. In the ocean sensing module, through the use of algorithms, such as adaptive and predictive control technology, the robustness and working life of the system can be improved. The wireless transceiver module should adapt to the data reduction/compression and cloud control algorithm update to reduce energy loss.

3.2.4. Resistance to biofouling and corrosion of OKEH

The degradation of OKEH is a highly complicated phenomenon because of their inherent extreme operating conditions, corrosive environment, and extended operations away from maintenance facilities. To further improve the durability of OKEH in harsh marine environment, it needs to investigate effects of biofouling and corrosion on the performance of OKEH and methods to resist them. Biofouling can interfere with transducer elements, materials, cover optical ports and clog bearings. Excessive biological attachment would vary the center of gravity, metacenter and draft of the OKEH, thus the hydrodynamic performance of OKEH would change. It is worth to note that there is still less systematic study on how the biofouling affects the hydrodynamic and electrical performance of OKEHs, particularly for the nanogenerators. Low-drag and low-adhesion surfaces are commonly utilized to resist biofouling [239]. At the same time, some works [61,62] show that the high-voltage electrical field generated by TENGs can also be used to prevent biofouling. For marine corrosion, it is known as a highly
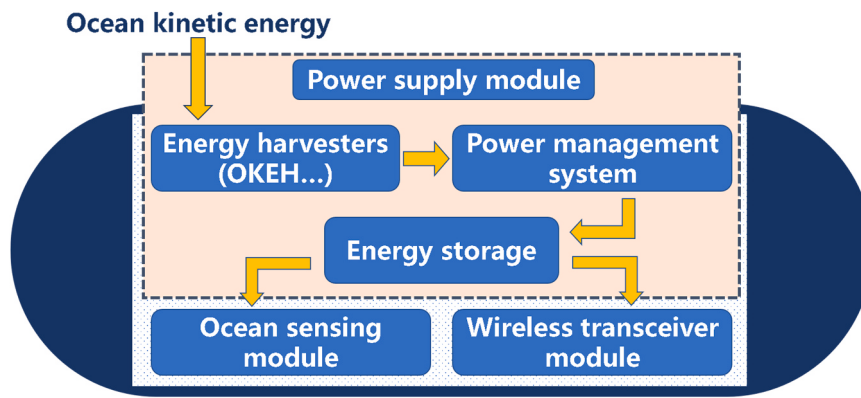
Fig. 22. General architecture of the integration of ocean sensor node and OKEH. This is an illustration of a self-powered sending system.

nonlinear process during the long exposures due to the involvement of numerous dependent/independent variables [240]. A multidisciplinary knowledge of material science, structural mechanics, electrochemistry, marine science and hydrodynamic is required. The methods to resist corrosion of OKEH may include sacrificial anodes, impressed current cathodic protection, various types of anti-fouling, anti-corrosive paints, and ultrasonic guided wave methods. Recently, based on the method of sacrificial anodes, TENG is adopted by using its electrical energy to protect the device from corrosion [63]. Thus, to ensure long-term survival of OKEH, it would be interesting and useful to investigate novel methods to protect OKEH structure and sensor node from biofouling and corrosion in the future.

4. Conclusions

In this study, the authors review the research status of OKEHs for powering distributed ocean sensors. Four major types of energy harvesters based on diverse mechanisms, including EMHs, EAHs, TENGs, and HHs, are introduced along with the corresponding representative progress in small-scale OKE harvesting. The four types of energy harvesters are analyzed and compared for energy conversion, device materials, output performance, marine sensor energy requirements, and application fields. The OKEH output enhancement, highly efficient power management system, integration of energy harvester, power management circuit, energy storage and sensor system, and resistance to biofouling and corrosion of OKEH are also proposed. The results suggest that OKEHs have an exceptional development prospective in powering ocean sensors. Based on the results, it has been concluded that TENG is the most appropriate technology for harvesting low-frequency, low-amplitude, random-direction wave energy. A hybridization of TENG with the other harvesters is highly recommended for harvesting high-entropy energy in ocean.

Meanwhile, it is worth noting that the ocean has entered the era of IoT. The underlying reason behind developing and utilizing marine resources is the real-time detection and collection of marine information. The construction of smart ocean requires more "energy of the new era" [100], to power the widespread marine equipment. From this perspective, the possible revolution in small-scale energy harvesting, ocean monitoring, marine resources exploitation, and self-powered sensor can further improve the marine safety and ecological resource utilization to a higher level that has never been achieved before.

Declaration of Competing Interest

The authors declare that they have no known competing financial interests or personal relationships that could have appeared to influence the work reported in this paper.

References

[1] Y. Zixuan, W. Zhifang, L. Chang, Research on marine environmental monitoring system based on the Internet of Things technology, in: 2016 IEEE International Conference on Electronic Information and Communication Technology (ICEICT), Harbin, China, 2016.

[2] C. Albaladejo, P. Sanchez, A. Iborra, F. Soto, J.A. Lopez, R. Torres, Wireless Sensor Networks for oceanographic monitoring: a systematic review, Sensors 10 (2010) 6948–6968, https://doi.org/10.3390/s100706948.

[3] W.K.G. Seah, Z.A. Eu, H.-P. Tan, Wireless sensor networks powered by ambient energy harvesting (WSN-HEAP) - Survey and challenges, in: 2009 1st International Conference on Wireless Communication, Vehicular Technology, Information Theory and Aerospace & Electronic Systems Technology, Aalborg, Denmark, 2009.

[4] H.K. Qureshi, S. Rizvi, M. Saleem, S.A. Khayam, V. Rakocevic, M. Rajarajan, Poly: A reliable and energy efficient topology control protocol for wireless sensor networks, Comput. Commun. 34 (2011) 1235–1242, https://doi.org/10.1016/j.comcom.2010.12.016.

[5] M. Prauzek, J. Konecny, M. Borová, K. Janošová, J. Hlavica, P. Musilek, Energy harvesting sources, storage devices and system topologies for environmental wireless sensor networks: a review, Sensors 18 (2018) 2446, https://doi.org/10.3390/s18082446.

[6] V. Radhakrishnan, W. Wu, IoT technology for smart water system, in: 2018 IEEE 20th International Conference on High Performance Computing and Communications; IEEE 16th International Conference on Smart City; IEEE 4th International Conference on Data Science and Systems (HPCC/SmartCity/DSS), 2018.

[7] A. Raj, D. Steingart, Review—power sources for the internet of things, J. Electrochem. Soc. 165 (2018) B3130–B3136, https://doi.org/10.1149/2.0181808jes.

[8] J. Tateson, C. Roadknight, A. Gonzalez, T. Khan, S. Fitz, I. Henning, N. Boyd, C. Vincent, I. Marshall, Real world issues in deploying a wireless sensor network for oceanography, in: Workshop on Real-world Wireless Sensor Networks REALWSN'05, Stockholm, Sweden, 2005.

[9] M. Iacono, S. Marrone, E. Romano, Adaptive monitoring of marine disasters with intelligent mobile sensor networks, in: Environmental Energy & Structural Monitoring Systems, Taranto, Italy, 2010.

[10] N. Wright, H.-K. Chan, Low-cost Internet of Things ocean observation, in: OCEANS 2016 MTS/IEEE Monterey, Monterey, CA, USA, 2016.

[11] M. Khalid, Z. Ullah, N. Ahmad, M. Arshad, B. Jan, Y. Cao, A. Adnan, A survey of routing issues and associated protocols in underwater wireless sensor networks, J. Sens. 2017 (2017) 1–17, https://doi.org/10.1155/2017/7539751.

[12] Y. Guo, Q. Han, J. Wang, X. Yu, Energy-aware localization algorithm for Ocean Internet of Things, Sens. Rev. 38 (2018) 129–136, https://doi.org/10.1108/sr-06-2017-0105.

[13] K. Awan, D.P.A. Shah, K. Iqbal, S. Gillani, W. Ahmad, Y. Nam, Underwater wireless sensor networks: a review of recent issues and challenges, Wirel. Commun. Mob. Comput. 2019 (2019) 1–20, https://doi.org/10.1155/2019/6470359.

[14] A. Piedra, F. Benitez-Capistros, F. Dominguez, A. Touhafi, Wireless Sensor Networks for Environmental Research: A Survey on Limitations and Challenges, in: Eurocon, Zagreb, Croatia, 2013.

[15] H. Lu, D. Wang, Y. Li, J. Li, X. Li, H. Kim, S. Serikawa, I. Humar, CONet: a cognitive ocean network, IEEE Wirel. Commun. 26 (2019) 90–96, https://doi.org/10.1109/mwc.2019.1800325.

[16] S. Kroger, R.J. Law, Sensing the sea, Trends Biotechnol. 23 (2005) 250–256, https://doi.org/10.1016/j.tibtech.2005.03.004.

[17] G. Xu, W. Shen, X. Wang, Applications of wireless sensor networks in marine environment monitoring: a survey, Sensors 14 (2014) 16932–16954, https://doi.org/10.3390/s140916932.

[18] D. Blidberg, R. Turner, S. Chappell, Autonomous underwater vehicles: current activities and research opportunities, Robot. Auton. Syst. 7 (1989) 2, https://doi.org/10.1016/0921-8890(91)90038-M.

[19] M.C. Domingo, An overview of the internet of underwater things, J. Netw. Comput. Appl. 35 (2012) 1879–1890, https://doi.org/10.1016/j.jnca.2012.07.012.

[20] X. Wang, J. Shang, Z. Luo, L. Tang, X. Zhang, J. Li, Reviews of power systems and environmental energy conversion for unmanned underwater vehicles, Renew. Sustain. Energy Rev. 16 (2012) 1958–1970, https://doi.org/10.1016/j.rser.2011.12.016.

[21] J. Aguzzi, M.M. Flexas, S. Flogel, C. Lo Iacono, M. Tangherlini, C. Costa, S. Marini, N. Bahamon, S. Martini, E. Fanelli, R. Danovaro, S. Stefanni, L. Thomsen, G. Riccobene, M. Hildebrandt, I. Masmitja, J. Del Rio, E.B. Clark, A. Branch, P. Weiss, A.T. Klesh, M.P. Schodlok, Exo-Ocean exploration with deep-sea sensor and platform technologies, Astrobiology 20 (2020) 897–915, https://doi.org/10.1089/ast.2019.2129.

[22] D. Eleftherakis, R. Vicen, Sensors to increase the security of underwater communication cables: a review of underwater monitoring sensors, Sensors 20 (2020) 737, https://doi.org/10.3390/s20030737.

[23] T. Qiu, Z. Zhao, T. Zhang, C. Chen, C.L.P. Chen, Underwater internet of things in smart ocean: system architecture and open issues, IEEE Trans. Ind. Inform. 16 (2020) 4297–4307, https://doi.org/10.1109/tii.2019.2946618.

[24] J. Yang, J. Wen, Y. Wang, B. Jiang, H. Wang, H. Song, Fog-based marine environmental information monitoring toward ocean of things, IEEE Internet Things 7 (2020) 4238–4247, https://doi.org/10.1109/jiot.2019.2946269.

[25] M. Zhu, T. He, C. Lee, Technologies toward next generation human machine interfaces: from machine learning enhanced tactile sensing to neuromorphic sensory systems, Appl. Phys. Rev. 7 (2020), 031305, https://doi.org/10.1063/5.0016485.

[26] C. Albaladejo, F. Soto, R. Torres, P. Sanchez, J.A. Lopez, A low-cost sensor buoy system for monitoring shallow marine environments, Sensors 12 (2012) 9613–9634, https://doi.org/10.3390/s120709613.

[27] P. Mueller, H. Thoss, L. Kaempf, A. Guntner, A buoy for continuous monitoring of Suspended Sediment Dynamics, Sensors 13 (2013) 13779–13801, https://doi.org/10.3390/s131013779.

[28] A. Lucas, R. Pinkel, M. Alford, Ocean wave energy for long endurance, broad bandwidth ocean monitoring, Oceanography 30 (2017) 126–127, https://doi.org/10.5670/oceanog.2017.232.

[29] M. Ayob, V. Castellucci, M. Göteman, J. Widén, J. Abrahamsson, J. Engström, R. Waters, Small-scale renewable energy converters for battery charging, JMSE 6 (2018) 26, https://doi.org/10.3390/jmse6010026.

[30] M. Marcelli, V. Piermattei, A. Madonia, U. Mainardi, Design and application of new low-cost instruments for marine environmental research, Sensors 14 (2014) 23348–23364, https://doi.org/10.3390/s141223348.

[31] F. Akhtar, M.H. Rehmani, Energy replenishment using renewable and traditional energy resources for sustainable wireless sensor networks: a review, Renew. Sustain. Energy Rev. 45 (2015) 769–784, https://doi.org/10.1016/j.rser.2015.02.021.

[32] Observation ROV system, ⟨http://www.robosea.org/rov.html⟩, 2020. (Accessed 1 March 2020).

[33] X. Xiang, Z. Niu, L. Lapierre, M. Zuo, Hybrid underwater robotic vehicles: the state-of-the-art and future trends, HKIE Trans. 22 (2015) 103–116.

[34] J. Yuh, M. West, Underwater robotics, Adv. Robot. 15 (2012) 609–639, https://doi.org/10.1163/156855301317033595.

[35] High-quality data buoy, ⟨https://www.ysi.com/File%20Library/Documents/Specification%20Sheets/DB600-Buoy-Specification-Sheet.pdf⟩, 2020. (Accessed 1 March 2020).

[36] Buoy automatic monitoring system, ⟨https://www.ysi.com/EMM150⟩, 2020. (Accessed 1 March 2020).

[37] D.L. Rudnick, R. Davis, C.C. Eriksen, D. Fratantoni, M.J. Perry, Underwater Gliders for Ocean Research, 38 (2004) 73–84. https://doi.org/10.4031/002533204787522703.

[38] Current profile, ⟨https://www.sontek.com/adp-acoustic-doppler-profiler/⟩, 2020. (Accessed 1 March 2020).

[39] Ultrasonic Thickness Gauge, ⟨https://www.cygnus-instruments.com/wp-content/uploads/2019/06/cygnus-mini-rov-mountable-data-sheet-iss5–1.pdf⟩, 2020. (Accessed 1 March 2020).

[40] Oxygen sensor, ⟨https://www.aanderaa.com/productsdetail.php?Oxygen-Sensors-2⟩, 2020. (Accessed 1 March 2020).

[41] Conductive sensor, ⟨https://www.aanderaa.com/productsdetail.php?Conductivity-sensor-9⟩, 2020. (Accessed 1 March 2020).

[42] Radiation, ⟨https://www.seabird.com/multispectral-radiometers/⟩, 2020. (Accessed 1 March 2020).

[43] Dissolved oxygen sensor, ⟨https://www.ysi.com/File%20Library/Documents/Manuals/ba76014-FDO-70x-IQ-YSI.PDF⟩, 2020. (Accessed 1 March 2020).

[44] Temperature sensor, ⟨https://www.aanderaa.com/productsdetail.php?Temperature-Sensor-12⟩, 2020. (Accessed 1 March 2020).

[45] Pressure sensor, ⟨https://www.aanderaa.com/productsdetail.php?Pressure-Sensor-11⟩, 2020. (Accessed 1 March 2020).

[46] Tide &Wave recorder, ⟨https://www.aanderaa.com/productsdetail.php?Wave-and-Tide-Sensor-13⟩, 2020. (Accessed 1 March 2020).

[47] Wave staff, ⟨http://oceansensorsystems.com/PDF/OSSI-010–002F.pdf⟩, 2020. (Accessed 1 March 2020).

[48] pHsensor, ⟨https://www.seabird.com/seafet-v2-ocean-pHsensor/product-downloads?id=54627921732⟩, 2020. (Accessed 1 March 2020).

[49] Chlorophyll sensor, ⟨https://www.ysi.com/File%20Library/Documents/Manuals/EXO_User_Manual_Deutsch.pdf⟩, 2020. (Accessed 1 March 2020).

[50] Nitrate, ⟨https://www.ysi.com/File%20Library/Documents/Manuals/EXO-User-Manual-Web.pdf⟩, 2020. (Accessed 1 March 2020).

[51] Glider Payload CTD, ⟨https://www.seabird.com/⟩, 2020. (Accessed 1 March 2020).

[52] Turbidity sensor, ⟨https://www.aanderaa.com/media/pdfs/d377_aanderaa_turbidity_sensor_4112.pdf⟩, 2020. (Accessed 1 March 2020).

[53] Wave Gauge, ⟨http://oceansensorsystems.com/PDF/OSSI-010–003C.pdf⟩, 2020. (Accessed 1 March 2020).

[54] Sonic Wave Sensor XB, ⟨http://oceansensorsystems.com/PDF/OSSI-010–035Sonic%20Wave%20Sensor%20XB.pdf⟩, 2020. (Accessed 1 March 2020).

[55] Wave Logger, ⟨http://oceansensorsystems.com/PDF/OSSI-010–004%2009–28-10.pdf⟩, 2020. (Accessed 1 March 2020).

[56] M. Sudhakar, A. Trishul, M. Doble, K. Suresh Kumar, S. Syed Jahan, D. Inbakandan, R.R. Viduthalai, V.R. Umadevi, P. Sriyutha Murthy, R. Venkatesan, Biofouling and biodegradation of polyolefins in ocean waters, Polym. Degrad. Stabil. 92 (2007) 1743–1752, https://doi.org/10.1016/j.polymdegradstab.2007.03.029.

[57] J. Jacquin, J. Cheng, C. Odobel, C. Pandin, P. Conan, M. Pujo-Pay, V. Barbe, A.L. Meistertzheim, J.F. Ghiglione, Microbial ecotoxicology of marine plastic debris: a review on colonization and biodegradation by the "Plastisphere", Front. Microbiol. 10 (2019) 865, https://doi.org/10.3389/fmicb.2019.00865.

[58] V. Martínez-Vicente, J.R. Clark, P. Corradi, S. Aliani, M. Arias, M. Bochow, G. Bonnery, M. Cole, A. Cózar, R. Donnelly, F. Echevarría, F. Galgani, S.P. Garaba, L. Goddijn-Murphy, L. Lebreton, H.A. Leslie, P.K. Lindeque, N. Maximenko, F.-R. Martin-Lauzer, D. Moller, P. Murphy, L. Palombi, V. Raimondi, J. Reisser, L. Romero, S.G.H. Simis, S. Sterckx, R.C. Thompson, K.N. Topouzelis, Ev van Sebille, J.M. Veiga, A.D. Vethaak, Measuring marine plastic debris from space: initial assessment of observation requirements, Remote Sens. 11 (2019) 2443, https://doi.org/10.3390/rs11202443.

[59] K. Pelegrini, T.G. Maraschin, R.N. Brandalise, D. Piazza, Study of the degradation and recyclability of polyethylene and polypropylene present in the marine environment, J. Appl. Polym. Sci. 136 (2019) 48215, https://doi.org/10.1002/app.48215.

[60] O. Langhamer, K. Haikonen, J.J.R. Sundberg, S.E. Reviews, Wave power—sustainable energy or environmentally costly? A review with special emphasis on linear wave energy converters, Renew. Sustain. Energy Rev. 14 (2010) 1329–1335.

[61] J.A. Callow, M.E. Callow, Trends in the development of environmentally friendly fouling-resistant marine coatings, Nat. Commun. 2 (2011) 244, https://doi.org/10.1038/ncomms1251.

[62] X.J. Zhao, J.J. Tian, S.Y. Kuang, H. Ouyang, L. Yan, Z.L. Wang, Z. Li, G. Zhu, Biocide-free antifouling on insulating surface by wave-driven triboelectrification-induced potential oscillation, Adv. Mater. Interfaces 3 (2016), 1600187.

[63] Z. Xuejiao, G. Zhu, Y. Fan, H. Yang Li, Z. Lin Wang, Triboelectric charging at the nanostructured solid/liquid interface for area-scalable wave energy conversion and its use in corrosion protection, ACS Nano 9 (2015) 7, https://doi.org/10.1021/acsnano.5b03093.

[64] L. Zhou, D. Liu, S. Li, X. Yin, C. Zhang, X. Li, C. Zhang, W. Zhang, X. Cao, J. Wang, Z.L. Wang, Effective removing of hexavalent chromium from wasted water by triboelectric nanogenerator driven self-powered electrochemical system – why pulsed DC is better than continuous DC? Nano Energy 64 (2019), 103915 https://doi.org/10.1016/j.nanoen.2019.103915.

[65] Q. Schiermeier, J. Tollefson, T. Scully, Electricity without carbon, Nature 454 (2008) 816–823.

[66] C. Knight, J. Davidson, S. Behrens, Energy options for wireless sensor nodes, Sensors 8 (2008) 8037–8066, https://doi.org/10.3390/s8128037.

[67] J. Tollefson, Power from the oceans: blue energy, Nature 508 (2014) 302–304.

[68] Z.L. Wang, Triboelectric nanogenerators as new energy technology and self-powered sensors - principles, problems and perspectives, Faraday Discuss. 176 (2014) 447–458, https://doi.org/10.1039/c4fd00159a.

[69] J. Scruggs, P. Jacob, Harvesting ocean wave energy, Science 323 (2009) 1176–1178.

[70] Z.L. Wang, T. Jiang, L. Xu, Toward the blue energy dream by triboelectric nanogenerator networks, Nano Energy 39 (2017) 9–23, https://doi.org/10.1016/j.nanoen.2017.06.035.

[71] J. Khan, G. Bhuyan, A. Moshref, K. Morison, J.H. Pease, J. Gurney, 2008 IEEE Power and Energy Society General Meeting - Conversion and Delivery of Electrical Energy in the 21st Century 2008, pp. 1–8.

[72] A.Fd.O. Falcão, Wave energy utilization: a review of the technologies, Renew. Sustain. Energy Rev. 14 (2010) 899–918, https://doi.org/10.1016/j.rser.2009.11.003.

[73] M. Melikoglu, Current status and future of ocean energy sources: a global review, Ocean Eng. 148 (2018) 563–573, https://doi.org/10.1016/j.oceaneng.2017.11.045.

[74] Z.L. Wang, Catch wave power in floating nets, Nature 542 (2017) 159–160.

[75] A.G.L. Borthwick, Marine renewable energy seascape, Engineering 2 (2016) 69–78, https://doi.org/10.1016/j.Eng.2016.01.011.

[76] C. Zheng, L. Shao, W. Shi, Q. Su, G. Lin, X. Li, X. Chen, An assessment of global ocean wave energy resources over the last 45 a, Acta Oceanol. Sin. 33 (2014) 92–101, https://doi.org/10.1007/s13131-014-0418-5.

[77] H. Chen, T. Tang, N. Ait-Ahmed, M.E.H. Benbouzid, M. Machmoum, M.E.-H. Zaim, Attraction, challenge and current status of marine current energy, IEEE Access 6 (2018) 12665–12685, https://doi.org/10.1109/access.2018.2795708.

[78] K.S.L. John Huckerby, W. Musial, T. Pontes, J. Torres-Martinez, Ocean Energy, renewable energy sources and climate change mitigation, 2011.

[79] Wave Energy, ⟨https://web.archive.org/web/20080627144946/http://www.oceanenergycouncil.com/content/view/10/13/⟩, 2008. (Accessed 23 August 2011).

[80] B. Czech, P.J.I.E.M.I. Bauer, Wave energy converter concepts: design challenges and classification, IEEE Ind. Electron. Mag. 6 (2012) 4–16.

[81] T.K.A. Brekken, A.v. Jouanne, H.Y. Han, Ocean wave energy overview and research at Oregon State University, in: 2009 IEEE Power Electronics and Machines in Wind Applications, Lincoln, NE, USA, 2009.

[82] A.J.R. Westwood, Ocean power: wave and tidal energy review, 5 (2004) 50–55.

[83] A.S. Bahaj, Marine current energy conversion: the dawn of a new era in electricity production, Philos. Trans. A Math. Phys. Eng. Sci. 371 (2013), 20120500, https://doi.org/10.1098/rsta.2012.0500.

[84] I.G. Bryden, S.J. Couch, ME1—marine energy extraction: tidal resource analysis, Renew. Energy 31 (2006) 133–139, https://doi.org/10.1016/j.renene.2005.08.012.

[85] I.R.E. Agency, Innovation Outlook Ocean Energy Technologies, 2020.

[86] W. Ritchie, K. Pond, E. Anthony, G. Maul, P. Wiberg, M. Hayes, A. Short, T. Healy, D. Barua, R. Charlier, G. Masselink, R. Fairbridge, D. Reed, W. Streever, Wave-Current Interaction, 2005, pp. 1052–1053.

[87] Z.L. Wang, Nanogenerators, self-powered systems, blue energy, piezotronics and piezo-phototronics – a recall on the original thoughts for coining these fields, Nano Energy 54 (2018) 477–483, https://doi.org/10.1016/j.nanoen.2018.09.068.

[88] Z.L. Wang, On Maxwell's displacement current for energy and sensors: the origin of nanogenerators, Mater. Today 20 (2017) 74–82, https://doi.org/10.1016/j.mattod.2016.12.001.

[89] P. Boccotti, On a new wave energy absorber, Ocean Eng. 30 (2003) 1191–1200, https://doi.org/10.1016/s0029-8018(02)00102-6.

[90] M. Leijon, O. Danielsson, M. Eriksson, K. Thorburn, H. Bernhoff, J. Isberg, J. Sundberg, I. Ivanova, E. Sjöstedt, O.J.R.E. Ågren, An electrical approach to wave energy conversion, Renew. Energy 31 (2006) 1309–1319, https://doi.org/10.1016/j.renene.2005.07.009.

[91] T.K.A. Brekken, A. von Jouanne, H. Yue Han, Ocean wave energy overview and research at Oregon State University, in: Power Electronics & Machines in Wind Applications, Lincoln, NE, USA, 2009.

[92] R.V. Chaplin, Seaweaver: a new surge-resonant wave energy converter, Renew. Energy 57 (2013) 662–670, https://doi.org/10.1016/j.renene.2011.04.009.

[93] I. López, J. Andreu, S. Ceballos, I. Martínez de Alegría, I. Kortabarria, Review of wave energy technologies and the necessary power-equipment, Renew. Sustain. Energy Rev. 27 (2013) 413–434, https://doi.org/10.1016/j.rser.2013.07.009.

[94] D. Khojasteh, R. Kamali, Evaluation of wave energy absorption by heaving point absorbers at various hot spots in Iran seas, Energy 109 (2016) 629–640, https://doi.org/10.1016/j.energy.2016.05.054.

[95] A. Uihlein, D.J.R. Magagna, S.E. Reviews, Wave and tidal current energy – a review of the current state of research beyond technology, Renew. Sustain. Energy Rev. 58 (2016) 1070–1081.

[96] H. Joe, H. Roh, H. Cho, S.-C. Yu, Development of a flap-type mooring-less wave energy harvesting system for sensor buoy, Energy 133 (2017) 851–863, https://doi.org/10.1016/j.energy.2017.05.143.

[97] N.Y. Sergiienko, B.S. Cazzolato, B. Ding, P. Hardy, M. Arjomandi, Performance comparison of the floating and fully submerged quasi-point absorber wave energy converters, Renew. Energy 108 (2017) 425–437, https://doi.org/10.1016/j.renene.2017.03.002.

[98] F.J. Arias, On resuspension and control of reservoir sediments by surface waves and point absorbers, J. Hydrol. 564 (2018) 773–784, https://doi.org/10.1016/j.jhydrol.2018.07.054.

[99] D. Yurchenko, P. Alevras, Parametric pendulum based wave energy converter, Mech. Syst. Signal Process. 99 (2018) 504–515, https://doi.org/10.1016/j.ymssp.2017.06.026.

[100] C. Wu, A.C. Wang, W. Ding, H. Guo, Z.L. Wang, Triboelectric nanogenerator: a foundation of the energy for the new era, Adv. Energy Mater. 9 (2019), 1802906, https://doi.org/10.1002/aenm.201802906.

[101] Z. Wang, Catch wave power in floating nets, Nature 542 (2017) 159–160, https://doi.org/10.1038/542159a.

[102] Y. Li, Q. Guo, M. Huang, X. Ma, Z. Chen, H. Liu, L. Sun, Study of an electromagnetic ocean wave energy harvester driven by an efficient swing body toward the self-powered ocean buoy application, IEEE Access 7 (2019) 129758–129769, https://doi.org/10.1109/access.2019.2937587.

[103] O.R. Chowdhury, H.-g Kim, D.-g Park, Y. Cho, C. Shin, J. Park, Development of a simple and innovative wave energy harvester suitable for ocean sensor network application, Int. J. Smart Home 9 (2015) 197–210, https://doi.org/10.14257/ijsh.2015.9.11.21.

[104] W. Ding, B. Song, Z. Mao, K. Wang, Experimental investigations on a low frequency horizontal pendulum ocean kinetic energy harvester for underwater mooring platforms, J. Mar. Sci. Technol. Jpn. 21 (2015) 359–367, https://doi.org/10.1007/s00773-015-0357-7.

[105] W. Ding, B. Song, M. Zhaoyong, K. Wang, Experimental investigation on an ocean kinetic energy harvester for underwater gliders, in: 2015 IEEE Energy Conversion Congress and Exposition, Montreal, QC, Canada, 2015.

[106] K. Yerrapragada, M.H. Ansari, M.A. Karami, Enhancing power generation of floating wave power generators by utilization of nonlinear roll-pitch coupling, Smart Mater. Struct. 26 (2017), 094003, https://doi.org/10.1088/1361-665X/aa7710.

[107] P.D. Mitcheson, E.M. Yeatman, G.K. Rao, A.S. Holmes, T.C. Green, Energy harvesting from human and machine motion for wireless electronic devices, Proc. IEEE 96 (2008) 1457–1486, https://doi.org/10.1109/jproc.2008.927494.

[108] H. Prahlad, R. Kornbluh, R. Pelrine, S. Stanford, J. Eckerle, S. Oh, Polymer power: dielectric elastomers and their applications in distributed actuation and power generation, in: Proceedings of ISSS, 2005.

[109] Y. Bar-Cohen, D.M. Opris, F. Carpi, M. Molberg, F. Nüesch, C. Löwe, C. Walder, B. Fischer, Dielectric elastomer materials for actuators and energy harvesting, in: Electroactive Polymer Actuators and Devices, San Diego, California, United States, 2011.

[110] S. Chiba, M. Waki, R. Kornbluh, R. Pelrine, Current status and future prospects of power generators using dielectric elastomers, Smart Mater. Struct. 20 (2011), 124006, https://doi.org/10.1088/0964-1726/20/12/124006.

[111] J. Maas, C. Graf, Dielectric elastomers for hydro power harvesting, Smart Mater. Struct. 21 (2012), 064006, https://doi.org/10.1088/0964-1726/21/6/064006.

[112] S.-K. Park, J. Ahn, J. Lee, S. Park, H.-M. Kim, K. Park, G. Hwang, M. Kim, S. Baek, G.-S. Byun, An ionic polymer metal composite based electrochemical conversion system in the ocean, Int. J. Electrochem. Sci. 9 (2014) 8067–8078.

[113] H.-M. Kim, Electroactive polymers for ocean kinetic energy harvesting: literature review and research needs, J. Ocean Eng. Mar. Energy 4 (2018) 343–365, https://doi.org/10.1007/s40722-018-0121-2.

[114] G. Thomson, D. Yurchenko, D.V. Val, Dielectric elastomers for energy harvesting, in: Energy Harvesting, 2018.

[115] K.M. Farinholt, N.A. Pedrazas, D.M. Schluneker, D.W. Burt, C.R. Farrar, An energy harvesting comparison of piezoelectric and ionically conductive polymers, J. Intell. Mater. Syst. Struct. 20 (2008) 633–642, https://doi.org/10.1177/1045389×08099604.

[116] C. Zheng, S. Shatara, T. Xiaobo, Modeling of biomimetic robotic fish propelled by an ionic polymer–metal composite caudal fin, IEEE ASME Trans. Mech. 15 (2010) 448–459, https://doi.org/10.1109/tmech.2009.2027812.

[117] R. Tiwari, K.J. Kim, IPMC as a mechanoelectric energy harvester: tailored properties, Smart Mater. Struct. 22 (2013), 015017, https://doi.org/10.1088/0964-1726/22/1/015017.

[118] S.R. Anton, H.A. Sodano, A review of power harvesting using piezoelectric materials (2003–2006), Smart Mater. Struct. 16 (2007) R1–R21, https://doi.org/10.1088/0964-1726/16/3/r01.

[119] M.S. Woo, K.H. Baek, J.H. Kim, S.B. Kim, D. Song, T.H. Sung, Relationship between current and impedance in piezoelectric energy harvesting system for water waves, J. Electroceram. 34 (2014) 180–184, https://doi.org/10.1007/s10832-014-9971-8.

[120] X.D. Xie, Q. Wang, N. Wu, Energy harvesting from transverse ocean waves by a piezoelectric plate, Int. J. Eng. Sci. 81 (2014) 41–48, https://doi.org/10.1016/j.ijengsci.2014.04.003.

[121] N. Wu, Q. Wang, X. Xie, Ocean wave energy harvesting with a piezoelectric coupled buoy structure, Appl. Ocean Res. 50 (2015) 110–118, https://doi.org/10.1016/j.apor.2015.01.004.

[122] Y. Han, Y. Feng, Z. Yu, W. Lou, H. Liu, A study on piezoelectric energy-harvesting wireless sensor networks deployed in a weak vibration environment, IEEE Sens. J. 17 (2017) 6770–6777, https://doi.org/10.1109/jsen.2017.2747122.

[123] Y.-m Na, H.-s Lee, J.-k Park, A study on piezoelectric energy harvester using kinetic energy of ocean, J. Mech. Sci. Technol. 32 (2018) 4747–4755, https://doi.org/10.1007/s12206-018-0922-1.

[124] G. Moretti, M. Santos Herran, D. Forehand, M. Alves, H. Jeffrey, R. Vertechy, M. Fontana, Advances in the development of dielectric elastomer generators for wave energy conversion, Renew. Sustain. Energy Rev. 117 (2020), 109430, https://doi.org/10.1016/j.rser.2019.109430.

[125] E. Aksel, J.L. Jones, Advances in lead-free piezoelectric materials for sensors and actuators, Sensors 10 (2010) 1935–1954, https://doi.org/10.3390/s100301935.

[126] K. Tao, J. Wu, A.G.P. Kottapalli, S.W. Lye, J. Miao, MEMS/NEMS-Enabled Vibrational Energy Harvesting for Self-Powered and Wearable Electronics, 2017, pp. 271–297.

[127] Z. Su, H. Wu, H. Chen, H. Guo, X. Cheng, Y. Song, X. Chen, H. Zhang, Digitalized self-powered strain gauge for static and dynamic measurement, Nano Energy 42 (2017) 129–137, https://doi.org/10.1016/j.nanoen.2017.10.004.

[128] T.Q. Trung, N.E. Lee, Flexible and stretchable physical sensor integrated platforms for wearable human-activity monitoringand personal healthcare, Adv. Mater. 28 (2016) 4338–4372, https://doi.org/10.1002/adma.201504244.

[129] X. Wen, W. Wu, C. Pan, Y. Hu, Q. Yang, Z. Lin Wang, Development and progress in piezotronics, Nano Energy 14 (2015) 276–295, https://doi.org/10.1016/j.nanoen.2014.10.037.

[130] C. Dagdeviren, Y. Shi, P. Joe, R. Ghaffari, G. Balooch, K. Usgaonkar, O. Gur, P. L. Tran, J.R. Crosby, M. Meyer, Y. Su, R. Chad Webb, A.S. Tedesco, M.J. Slepian, Y. Huang, J.A. Rogers, Conformal piezoelectric systems for clinical and experimental characterization of soft tissue biomechanics, Nat. Mater. 14 (2015) 728–736, https://doi.org/10.1038/nmat4289.

[131] E.V. White, J. Rastegar, C. Pereira, H.L. Nguyen, Piezoelectric-based power sources for harvesting energy from platforms with low-frequency vibration, in: Smart Structures and Materials 2006: Industrial and Commercial Applications of Smart Structures Technologies, San Diego, California, United States, 2006.

[132] A. Jbaily, R.W. Yeung, Piezoelectric devices for ocean energy: a brief survey, J. Ocean Eng. Mar. Energy 1 (2015) 101–118, https://doi.org/10.1007/s40722-014-0008-9.

[133] H. Kawai, The piezoelectricity of poly (vinylidene fluoride), Jpn. J. Appl. Phys. 8 (1969) 975–976, https://doi.org/10.1143/jjap.8.975.

[134] D. Guyomar, A. Badel, E. Lefeuvre, C. Richard, Toward energy harvesting using active materials and conversion improvement by nonlinear processing, IEEE Trans. Ultrason. Ferroelectr. Freq. Control 52 (2005) 584–595, https://doi.org/10.1109/TUFFC.2005.1428041.

[135] Y.C. Shu, I.C. Lien, Efficiency of energy conversion for a piezoelectric power harvesting system, J. Micromech. Microeng. 16 (2006) 2429–2438, https://doi.org/10.1088/0960-1317/16/11/026.

[136] C.D. Richards, M.J. Anderson, D.F. Bahr, R.F. Richards, Efficiency of energy conversion for devices containing a piezoelectric component, J. Micromech. Microeng. 14 (2004) 717–721, https://doi.org/10.1088/0960-1317/14/5/009.

[137] G.W. Taylor, J.R. Burns, S.A. Kammann, W.B. Powers, T.R. Welsh, The Energy Harvesting Eel: a small subsurface ocean/river power generator, IEEE J. Ocean. Eng. 26 (2001) 539–547.

[138] M.M. Bernitsas, K. Raghavan, Y. Ben-Simon, E.M.H. Garcia, VIVACE (Vortex Induced Vibration Aquatic Clean Energy): a new concept in generation of clean and renewable energy from fluid flow, J. Offshore Mech. Arct. 130 (2008), 041101, https://doi.org/10.1115/1.2957913.

[139] H.D. Akaydın, N. Elvin, Y. Andreopoulos, Wake of a cylinder: a paradigm for energy harvesting with piezoelectric materials, Exp. Fluids 49 (2010) 291–304, https://doi.org/10.1007/s00348-010-0871-7.

[140] Y. Chen, X. Mu, T. Wang, W. Ren, Y. Yang, Z.L. Wang, C. Sun, A.Y. Gu, Flutter phenomenon in flow driven energy harvester-a unified theoretical model for "Stiff" and "Flexible" materials, Sci. Rep. 6 (2016) 35180, https://doi.org/10.1038/srep35180.

[141] Y. Yu, Y. Liu, Flapping dynamics of a piezoelectric membrane behind a circular cylinder, J. Fluid Struct. 55 (2015) 347–363, https://doi.org/10.1016/j.jfluidstructs.2015.03.009.

[142] J.Z. Gul, K.Y. Su, K.H. Choi, Fully 3D printed multi-material soft bio-inspired whisker sensor for underwater-induced vortex detection, Soft Robot. 5 (2018) 122–132, https://doi.org/10.1089/soro.2016.0069.

[143] J. Wang, L. Geng, L. Ding, H. Zhu, D. Yurchenko, The state-of-the-art review on energy harvesting from flow-induced vibrations, Appl. Energy 267 (2020), 114902, https://doi.org/10.1016/j.apenergy.2020.114902.

[144] H. Mutsuda, Y. Tanaka, R. Patel, Y. Doi, Y. Moriyama, Y. Umino, A painting type of flexible piezoelectric device for ocean energy harvesting, Appl. Ocean Res. 68 (2017) 182–193, https://doi.org/10.1016/j.apor.2017.08.008.

[145] W.S. Hwang, J.H. Ahn, S.Y. Jeong, H.J. Jung, S.K. Hong, J.Y. Choi, J.Y. Cho, J. H. Kim, T.H. Sung, Design of piezoelectric ocean-wave energy harvester using sway movement, Sens. Actuators A Phys. 260 (2017) 191–197, https://doi.org/10.1016/j.sna.2017.04.026.

[146] H. Mutsuda, R. Watanabe, M. Hirata, Y. Doi, Y. Tanaka, Elastic floating unit with piezoelectric device for harvesting ocean wave energy, in: ASME 2012 International Conference on Ocean, Offshore and Arctic Engineering, Rio de Janeiro, Brazil, 2012.

[147] H. Mutsuda, Y. Doi, Numerical simulation of dynamic response of structure caused by wave impact pressure using an Eulerian scheme with Lagrangian particles, in: ASME 2009 28th International Conference on Ocean, Offshore and Arctic Engineering, Honolulu, Hawaii, USA, 2009.

[148] H. Mutsuda, Y. Tanaka, R. Patel, Y. Doi, Harvesting flow-induced vibration using a highly flexible piezoelectric energy device, Appl. Ocean Res. 68 (2017) 39–52.

[149] R. Murray, J. Rastegar, Novel two-stage piezoelectric-based ocean wave energy harvesters for moored or unmoored buoys, in: The International Symposium On: Smart Structures and Materials & Nondestructive Evaluation and Health Monitoring, San Diego, CA, 2009.

[150] G.K. Ottman, H.F. Hofmann, A.C. Bhatt, G.A. Lesieutre, Adaptive piezoelectric energy harvesting circuit for wireless remote power supply, IEEE Trans. Power Electron. 17 (2002) 669–676, https://doi.org/10.1109/tpel.2002.802194.

[151] G.K. Ottman, H.F. Hofmann, G.A. Lesieutre, Optimized piezoelectric energy harvesting circuit using step-down converter in discontinuous conduction mode, IEEE Trans. Power Electron. 18 (2003) 696–703, https://doi.org/10.1109/tpel.2003.809379.

[152] H. Sodano, G. Park, D. Inman, Estimation of electric charge output for piezoelectric energy harvesting, Strain 40 (2004) 49–58, https://doi.org/10.1111/j.1475-1305.2004.00120.x.

[153] E. Lefeuvre, D. Audigier, C. Richard, D. Guyomar, Buck-boost converter for sensorless power optimization of piezoelectric energy harvester, IEEE Trans. Power Electron. 22 (2007) 2018–2025, https://doi.org/10.1109/tpel.904230.

[154] X. Wang, S. Niu, Y. Yin, F. Yi, Z. You, Z.L. Wang, Enhanced power output of a triboelectric nanogenerator composed of electrospun nanofiber mats doped with graphene oxide, Sci. Rep. 5 (2015) 13942, https://doi.org/10.1002/aenm.201501467.

[155] Z.L. Wang, Triboelectric nanogenerators as new energy technology for self-powered systems and as active mechanical and chemical sensors, ACS Nano 7 (2013) 9533–9557.

[156] M. Xu, T. Zhao, C. Wang, S.L. Zhang, Z. Li, X. Pan, Z.L. Wang, High power density tower-like triboelectric nanogenerator for harvesting arbitrary directional water

[157] wave energy, ACS Nano 13 (2019) 1932–1939, https://doi.org/10.1021/acsnano.8b08274.

[157] S.S.K. Mallineni, H. Behlow, R. Podila, A.M. Rao, A low-cost approach for measuring electrical load currents in triboelectric nanogenerators, Nanotechnol. Rev. 7 (2018) 149–156, https://doi.org/10.1515/ntrev-2017-0178.

[158] Y. Bai, L. Xu, C. He, L. Zhu, X. Yang, T. Jiang, J. Nie, W. Zhong, Z.L. Wang, High-performance triboelectric nanogenerators for self-powered, in-situ and real-time water quality mapping, Nano Energy 66 (2019), 104117, https://doi.org/10.1016/j.nanoen.2019.104117.

[159] J. Chen, W. Tang, K. Han, L. Xu, B. Chen, T. Jiang, Z.L. Wang, Bladeless-turbine-based triboelectric nanogenerator for fluid energy harvesting and self-powered fluid gauge, Adv. Mater. Technol. 4 (2019), 1800560, https://doi.org/10.1002/admt.201800560.

[160] J. Chung, D. Heo, G. Shin, D. Choi, K. Choi, D. Kim, S. Lee, Enhanced immobilization of Prussian blue through hydrogel formation by polymerization of acrylic acid for radioactive cesium adsorption, Sci. Rep. 9 (2019) 16334, https://doi.org/10.1002/aenm.201901731.

[161] X. Yang, S. Chan, L. Wang, W.A. Daoud, Water tank triboelectric nanogenerator for efficient harvesting of water wave energy over a broad frequency range, Nano Energy 44 (2018) 388–398, https://doi.org/10.1016/j.nanoen.2017.12.025.

[162] M. Mariello, F. Guido, V.M. Mastronardi, M.T. Todaro, D. Desmaële, M. De Vittorio, Nanogenerators for harvesting mechanical energy conveyed by liquids, Nano Energy 57 (2019) 141–156, https://doi.org/10.1016/j.nanoen.2018.12.027.

[163] M. Xu, P. Wang, Y.-C. Wang, S.L. Zhang, A.C. Wang, C. Zhang, Z. Wang, X. Pan, Z. L. Wang, A soft and robust spring based triboelectric nanogenerator for harvesting arbitrary directional vibration energy and self-powered vibration sensing, Adv. Energy Mater. 8 (2018), 1702432, https://doi.org/10.1002/aenm.201702432.

[164] L. Xu, T. Jiang, P. Lin, J.J. Shao, C. He, W. Zhong, X.Y. Chen, Z.L. Wang, Coupled triboelectric nanogenerator networks for efficient water wave energy harvesting, ACS Nano 12 (2018) 1849–1858, https://doi.org/10.1021/acsnano.7b08674.

[165] L. Xu, T.Z. Bu, X.D. Yang, C. Zhang, Z.L. Wang, Ultrahigh charge density realized by charge pumping at ambient conditions for triboelectric nanogenerators, Nano Energy 49 (2018) 625–633, https://doi.org/10.1016/j.nanoen.2018.05.011.

[166] T.X. Xiao, T. Jiang, J.X. Zhu, X. Liang, L. Xu, J.J. Shao, C.L. Zhang, J. Wang, Z. L. Wang, Silicone-based triboelectric nanogenerator for water wave energy harvesting, ACS Appl. Mater. Interfaces 10 (2018) 3616–3623, https://doi.org/10.1021/acsami.7b17239.

[167] S.-J. Park, S. Kim, M.-L. Seol, S.-B. Jeon, I.-W. Tcho, D. Kim, Y.-K. Choi, A multi-directional wind based triboelectric generator with investigation of frequency effects, Extrem. Mech. Lett. 19 (2018) 46–53, https://doi.org/10.1016/j.eml.2017.12.009.

[168] L. Pan, J. Wang, P. Wang, R. Gao, Y.-C. Wang, X. Zhang, J.-J. Zou, Z.L. Wang, Liquid-FEP-based U-tube triboelectric nanogenerator for harvesting water-wave energy, Nano Res. 11 (2018) 4062–4073, https://doi.org/10.1007/s12274-018-1989-9.

[169] G. Liu, J. Chen, Q. Tang, L. Feng, H. Yang, J. Li, Y. Xi, X. Wang, C. Hu, Wireless electric energy transmission through various isolated solid media based on triboelectric nanogenerator, Adv. Energy Mater. 8 (2018), 1703086, https://doi.org/10.1002/aenm.201703086.

[170] Q. Jiang, C. Wu, Z. Wang, A.C. Wang, J.-H. He, Z.L. Wang, H.N. Alshareef, MXene electrochemical microsupercapacitor integrated with triboelectric nanogenerator as a wearable self-charging power unit, Nano Energy 45 (2018) 266–272, https://doi.org/10.1016/j.nanoen.2018.01.004.

[171] X.X. Zhu, X.S. Meng, S.Y. Kuang, X.D. Wang, C.F. Pan, G. Zhu, Z.L. Wang, Triboelectrification-enabled touch sensing for self-powered position mapping and dynamic tracking by a flexible and area-scalable sensor array, Nano Energy 41 (2017) 387–393, https://doi.org/10.1016/j.nanoen.2017.09.025.

[172] H. Xue, Q. Yang, D. Wang, W. Luo, W. Wang, M. Lin, D. Liang, Q. Luo, A wearable pyroelectric nanogenerator and self-powered breathing sensor, Nano Energy 38 (2017) 147–154, https://doi.org/10.1016/j.nanoen.2017.05.056.

[173] M. Xu, Y.-C. Wang, S.L. Zhang, W. Ding, J. Cheng, X. He, P. Zhang, Z. Wang, X. Pan, Z.L. Wang, An aeroelastic flutter based triboelectric nanogenerator as a self-powered active wind speed sensor in harsh environment, Extrem. Mech. Lett. 15 (2017) 122–129, https://doi.org/10.1016/j.eml.2017.07.005.

[174] Y. Xi, J. Wang, Y. Zi, X. Li, C. Han, X. Cao, C. Hu, Z. Wang, High efficient harvesting of underwater ultrasonic wave energy by triboelectric nanogenerator, Nano Energy 38 (2017) 101–108, https://doi.org/10.1016/j.nanoen.2017.04.053.

[175] F. Xi, Y. Pang, W. Li, T. Jiang, L. Zhang, T. Guo, G. Liu, C. Zhang, Z.L. Wang, Universal power management strategy for triboelectric nanogenerator, Nano Energy 37 (2017) 168–176, https://doi.org/10.1016/j.nanoen.2017.05.027.

[176] C. Wu, R. Liu, J. Wang, Y. Zi, L. Lin, Z.L. Wang, A spring-based resonance coupling for hugely enhancing the performance of triboelectric nanogenerators for harvesting low-frequency vibration energy, Nano Energy 32 (2017) 287–293, https://doi.org/10.1016/j.nanoen.2016.12.061.

[177] J. Wang, C. Wu, Y. Dai, Z. Zhao, A. Wang, T. Zhang, Z.L. Wang, Achieving ultrahigh triboelectric charge density for efficient energy harvesting, Nat. Commun. 8 (2017) 88, https://doi.org/10.1038/s41467-017-00131-4.

[178] H. Zou, L. Guo, H. Xue, Y. Zhang, X. Shen, X. Liu, P. Wang, X. He, G. Dai, P. Jiang, H. Zheng, B. Zhang, C. Xu, Z.L. Wang, Quantifying and understanding the triboelectric series of inorganic non-metallic materials, Nat. Commun. 11 (2020) 2093, https://doi.org/10.1038/s41467-020-15926-1.

[180] B. Shi, Z. Li, Y. Fan, Implantable energy-harvesting devices, Adv. Mater. 30 (2018), 1801511, https://doi.org/10.1002/adma.201801511.

[182] X. Zhang, M. Yu, Z. Ma, H. Ouyang, Y. Zou, S.L. Zhang, H. Niu, X. Pan, M. Xu, Z. Li, Z.L. Wang, Self-powered distributed water level sensors based on liquid–solid triboelectric nanogenerators for ship draft detecting, Adv. Funct. Mater. 29 (2019), 1900327, https://doi.org/10.1002/adfm.201900327.

[183] X. Yang, L. Xu, P. Lin, W. Zhong, Y. Bai, J. Luo, J. Chen, Z.L. Wang, Macroscopic self-assembly network of encapsulated high-performance triboelectric nanogenerators for water wave energy harvesting, Nano Energy 60 (2019) 404–412, https://doi.org/10.1016/j.nanoen.2019.03.054.

[184] J. Wang, L. Pan, H. Guo, B. Zhang, R. Zhang, Z. Wu, C. Wu, L. Yang, R. Liao, Z. L. Wang, Rational structure optimized hybrid nanogenerator for highly efficient water wave energy harvesting, Adv. Energy Mater. 9 (2019), 1802892, https://doi.org/10.1002/aenm.201802892.

[185] J. Luo, Z.L. Wang, Recent advances in triboelectric nanogenerator based self-charging power systems, Energy Storage Mater. 23 (2019) 617–628, https://doi.org/10.1016/j.ensm.2019.03.009.

[186] X. Liang, T. Jiang, G. Liu, T. Xiao, L. Xu, W. Li, F. Xi, C. Zhang, Z.L. Wang, Triboelectric nanogenerator networks integrated with power management module for water wave energy harvesting, Adv. Funct. Mater. 29 (2019), 1807241, https://doi.org/10.1002/adfm.201807241.

[187] S.L. Zhang, M. Xu, C. Zhang, Y.-C. Wang, H. Zou, X. He, Z. Wang, Z.L. Wang, Rationally designed sea snake structure based triboelectric nanogenerators for effectively and efficiently harvesting ocean wave energy with minimized water screening effect, Nano Energy 48 (2018) 421–429, https://doi.org/10.1016/j.nanoen.2018.03.062.

[188] M. Xu, S. Wang, S.L. Zhang, W. Ding, P.T. Kien, C. Wang, Z. Li, X. Pan, Z.L. Wang, A highly-sensitive wave sensor based on liquid-solid interfacing triboelectric nanogenerator for smart marine equipment, Nano Energy 57 (2019) 574–580, https://doi.org/10.1016/j.nanoen.2018.12.041.

[189] Q. Shi, H. Wang, H. Wu, C. Lee, Self-powered triboelectric nanogenerator buoy ball for applications ranging from environment monitoring to water wave energy farm, Nano Energy 40 (2017) 203–213, https://doi.org/10.1016/j.nanoen.2017.08.018.

[190] Z. Zhang, D. Jiang, J. Zhao, G. Liu, T. Bu, C. Zhang, Z.L. Wang, Tribovoltaic effect on metal–semiconductor interface for direct-current low-impedance triboelectric nanogenerators, Adv. Energy Mater. 10 (2020), 1903713, https://doi.org/10.1002/aenm.201903713.

[191] W. Zhang, G. Gu, H. Qin, S. Li, W. Shang, T. Wang, B. Zhang, P. Cui, J. Guo, F. Yang, G. Cheng, Z. Du, Measuring the actual voltage of a triboelectric nanogenerator using the non-grounded method, Nano Energy 77 (2020), 105108, https://doi.org/10.1016/j.nanoen.2020.105108.

[192] H.J. Yoon, M. Kang, W. Seung, S.S. Kwak, J. Kim, H.T. Kim, S.W. Kim, Microdischarge-based direct current triboelectric nanogenerator via accumulation of triboelectric charge in atmospheric condition, Adv. Energy Mater. 10 (2020), 2000730, https://doi.org/10.1002/aenm.202000730.

[193] Z. Wu, T. Cheng, Z.L. Wang, Self-powered sensors and systems based on nanogenerators, Sensors 20 (2020) 2925, https://doi.org/10.3390/s20102925.

[194] F. Wen, Z. Sun, T. He, Q. Shi, M. Zhu, Z. Zhang, L. Li, T. Zhang, C. Lee, Machine learning glove using self-powered conductive superhydrophobic triboelectric textile for gesture recognition in VR/AR applications, Adv. Sci. 7 (2020), 2000261, https://doi.org/10.1002/advs.202000261.

[195] Z.L. Wang, Triboelectric nanogenerator (TENG)—sparking an energy and sensor revolution, Adv. Energy Mater. 10 (2020), 2000137, https://doi.org/10.1002/aenm.202000137.

[196] Z.L. Wang, On the first principle theory of nanogenerators from Maxwell's equations, Nano Energy 68 (2020), 104272, https://doi.org/10.1016/j.nanoen.2019.104272.

[197] Z. Wang, Y. Yu, Y. Wang, X. Lu, T. Cheng, G. Bao, Z.L. Wang, Magnetic flap-type difunctional sensor for detecting pneumatic flow and liquid level based on triboelectric nanogenerator, ACS Nano 14 (2020) 5981–5987, https://doi.org/10.1021/acsnano.0c01436.

[198] Q. Wang, H.-X. Zou, L.-C. Zhao, M. Li, K.-X. Wei, L.-P. Huang, W.-M. Zhang, A synergetic hybrid mechanism of piezoelectric and triboelectric for galloping wind energy harvesting, Appl. Phys. Lett. 117 (2020), 043902, https://doi.org/10.1063/5.0014484.

[199] F.R. Fan, W. Tang, Z.L. Wang, Flexible nanogenerators for energy harvesting and self-powered electronics, Adv. Mater. 28 (2016) 4283–4305, https://doi.org/10.1002/adma.201504299.

[200] X. Li, J. Tao, X. Wang, J. Zhu, C. Pan, Z.L. Wang, Networks of high performance triboelectric nanogenerators based on liquid-solid interface contact electrification for harvesting low-frequency blue energy, Adv. Energy Mater. 8 (2018), 1800705, https://doi.org/10.1002/aenm.201800705.

[201] L. Xu, Y. Pang, C. Zhang, T. Jiang, X. Chen, J. Luo, W. Tang, X. Cao, Z.L. Wang, Integrated triboelectric nanogenerator array based on air-driven membrane structures for water wave energy harvesting, Nano Energy 31 (2017) 351–358, https://doi.org/10.1016/j.nanoen.2016.11.037.

[202] S. Wang, L. Lin, Z.L. Wang, Triboelectric nanogenerators as self-powered active sensors, Nano Energy 11 (2015) 436–462, https://doi.org/10.1016/j.nanoen.2014.10.034.

[203] J. Shao, M. Willatzen, Z. Wang, Theoretical modeling of triboelectric nanogenerators (TENGs), J. Appl. Phys. 128 (2020), 111101, https://doi.org/10.1063/5.0020961.

[204] C. Rodrigues, D. Nunes, D. Clemente, N. Mathias, J.M. Correia, P. Rosa-Santos, F. Taveira-Pinto, T. Morais, A. Pereira, J. Ventura, Emerging triboelectric nanogenerators for ocean wave energy harvesting: state of the art and future perspectives, Energy Environ. Sci. 13 (2020) 2657–2683, https://doi.org/10.1039/D0EE01258K.

[205] C. Rodrigues, D. Nunes, D. Clemente, N. Mathias, J. Correia, P. Santos, F. Taveira-Pinto, T. Morais, A. Pereira, J. Ventura, Emerging triboelectric nanogenerators for ocean wave energy harvesting: state of the art and future perspectives, Energy Environ. Sci. 13 (2020) 2657–2683, https://doi.org/10.1039/D0EE01258K.

[206] T.X. Xiao, X. Liang, T. Jiang, L. Xu, J.J. Shao, J.H. Nie, Y. Bai, W. Zhong, Z. L. Wang, Spherical triboelectric nanogenerators based on spring-assisted multilayered structure for efficient water wave energy harvesting, Adv. Funct. Mater. 28 (2018), 1802634, https://doi.org/10.1002/adfm.201802634.

[207] P. Cheng, H. Guo, Z. Wen, C. Zhang, X. Yin, X. Li, D. Liu, W. Song, X. Sun, J. Wang, Z.L. Wang, Largely enhanced triboelectric nanogenerator for efficient harvesting of water wave energy by soft contacted structure, Nano Energy 57 (2019) 432–439, https://doi.org/10.1016/j.nanoen.2018.12.054.

[208] Z. Xuejiao, G. Zhu, Y. Fan, H. Yang Li, Z. Lin Wang, Triboelectric charging at the nanostructured solid/liquid interface for area-scalable wave energy conversion and its use in corrosion protection, 9 (2015). https://doi.org/10.1021/acsnano.5b03093.

[209] Y. Zi, S. Niu, J. Wang, Z. Wen, W. Tang, Z.L. Wang, Standards and figure-of-merits for quantifying the performance of triboelectric nanogenerators, Nat. Commun. 6 (2015) 8376, https://doi.org/10.1038/ncomms9376.

[210] W. Zhong, L. Xu, X. Yang, W. Tang, J. Shao, B. Chen, Z.L. Wang, Open-book-like triboelectric nanogenerators based on low-frequency roll-swing oscillators for wave energy harvesting, Nanoscale 11 (2019) 7199–7208, https://doi.org/10.1039/c8nr09978b.

[211] Y.C. Lai, Y.C. Hsiao, H.M. Wu, Z.L. Wang, Waterproof fabric-based multifunctional triboelectric nanogenerator for universally harvesting energy from raindrops, wind, and human motions and as self-powered sensors, Adv. Sci. 6 (2019), 1801883, https://doi.org/10.1002/advs.201801883.

[212] R. Lei, H. Zhai, J. Nie, W. Zhong, Y. Bai, X. Liang, L. Xu, T. Jiang, X. Chen, Z. L. Wang, Butterfly-inspired triboelectric nanogenerators with spring-assisted linkage structure for water wave energy harvesting, Adv. Mater. Technol. 4 (2019), 1800514, https://doi.org/10.1002/admt.201800514.

[213] W. Liu, Z. Wang, G. Wang, G. Liu, J. Chen, X. Pu, Y. Xi, X. Wang, H. Guo, C. Hu, Z. L. Wang, Integrated charge excitation triboelectric nanogenerator, Nat. Commun. 10 (2019) 1426, https://doi.org/10.1038/s41467-019-09464-8.

[214] X. Wen, W. Yang, Q. Jing, Z.L. Wang, Harvesting broadband kinetic impact energy from mechanical triggering/vibration and water waves, ACS Nano 8 (2014) 7405–7412.

[215] S. Niu, Y.S. Zhou, S. Wang, Y. Liu, L. Lin, Y. Bando, Z.L. Wang, Simulation method for optimizing the performance of an integrated triboelectric nanogenerator energy harvesting system, Nano Energy 8 (2014) 150–156, https://doi.org/10.1016/j.nanoen.2014.05.018.

[216] S. Wang, Y. Xie, S. Niu, L. Lin, Z.L. Wang, Freestanding triboelectric-layer-based nanogenerators for harvesting energy from a moving object or human motion in contact and non-contact modes, Adv. Mater. 26 (2014) 2818–2824, https://doi.org/10.1002/adma.201305303.

[217] Z.H. Lin, G. Cheng, S. Lee, K.C. Pradel, Z.L. Wang, Harvesting water drop energy by a sequential contact-electrification and electrostatic-induction process, Adv. Mater. 26 (2014) 4690–4696, https://doi.org/10.1002/adma.201400373.

[218] G. Liu, L. Xiao, C. Chen, W. Liu, X. Pu, Z. Wu, C. Hu, Z.L. Wang, Power cables for triboelectric nanogenerator networks for large-scale blue energy harvesting, Nano Energy 75 (2020), 104975, https://doi.org/10.1016/j.nanoen.2020.104975.

[219] T. Jiang, H. Pang, J. An, P. Lu, Y. Feng, X. Liang, W. Zhong, Z.L. Wang, Robust swing-structured triboelectric nanogenerator for efficient blue energy harvesting, Adv. Energy Mater. 10 (2020), 2000064, https://doi.org/10.1002/aenm.202000064.

[220] F. Xi, Y. Pang, G. Liu, S. Wang, W. Li, C. Zhang, Z.L. Wang, Self-powered intelligent buoy system by water wave energy for sustainable and autonomous wireless sensing and data transmission, Nano Energy 61 (2019) 1–9, https://doi.org/10.1016/j.nanoen.2019.04.026.

[221] X. Liang, T. Jiang, G. Liu, Y. Feng, C. Zhang, Z.L. Wang, Spherical triboelectric nanogenerator integrated with power management module for harvesting multidirectional water wave energy, Energy Environ. Sci. 13 (2020) 277–285, https://doi.org/10.1039/c9ee03258d.

[222] Z. Wen, H. Guo, Y. Zi, M.-H. Yeh, X. Wang, J. Deng, J. Wang, S. Li, C. Hu, L. Zhu, Z.L. Wang, Harvesting broad frequency band blue energy by a triboelectric–electromagnetic hybrid nanogenerator, ACS Nano 10 (2016) 6526–6534, https://doi.org/10.1021/acsnano.6b03293.

[223] Z. Wu, H. Guo, W. Ding, Y.C. Wang, L. Zhang, Z.L. Wang, A hybridized triboelectric-electromagnetic water wave energy harvester based on a magnetic sphere, ACS Nano 13 (2019) 2349–2356, https://doi.org/10.1021/acsnano.8b09088.

[224] X. Chen, L. Gao, J. Chen, S. Lu, H. Zhou, T. Wang, A. Wang, Z. Zhang, S. Guo, X. Mu, C. Wang, Y. Yang, A chaotic pendulum triboelectric-electromagnetic hybridized nanogenerator for wave energy scavenging and self-powered wireless sensing system, Nano Energy 69 (2020), 104440, https://doi.org/10.1016/j.nanoen.2019.104440.

[225] H. Shao, Z. Wen, P. Cheng, N. Sun, Q. Shen, C. Zhou, M. Peng, Y. Yang, X. Xie, X. Sun, Multifunctional power unit by hybridizing contact-separate triboelectric nanogenerator, electromagnetic generator and solar cell for harvesting blue energy, Nano Energy 39 (2017) 608–615, https://doi.org/10.1016/j.nanoen.2017.07.045.

[226] X. Wang, Z. Wen, H. Guo, C. Wu, X. He, L. Lin, X. Cao, Z.L. Wang, Fully packaged blue energy harvester by hybridizing a rolling triboelectric nanogenerator and an electromagnetic generator, ACS Nano 10 (2016) 11369–11376, https://doi.org/10.1021/acsnano.6b06622.

[227] X. Liang, T. Jiang, Y. Feng, P. Lu, J. An, Z.L. Wang, Triboelectric nanogenerator network integrated with charge excitation circuit for effective water wave energy harvesting, Adv. Energy Mater. 10 (2020), 2002123, https://doi.org/10.1002/aenm.202002123.

[228] Z. Saadatnia, E. Asadi, H. Askari, E. Esmailzadeh, H.E. Naguib, A heaving point absorber-based triboelectric-electromagnetic wave energy harvester: an efficient approach toward blue energy, Int. J. Energy Res. 42 (2018) 2431–2447, https://doi.org/10.1002/er.4024.

[229] Y. Feng, X. Liang, J. An, T. Jiang, Z.L. Wang, Soft-contact cylindrical triboelectric-electromagnetic hybrid nanogenerator based on swing structure for ultra-low frequency water wave energy harvesting, Nano Energy 81 (2021), 105625, https://doi.org/10.1016/j.nanoen.2020.105625.

[230] L. Liu, Q. Shi, C. Lee, Cluster-mining: an approach for determining core structures of metallic nanoparticles from atomic pair distribution function data, Acta Crystallogr. Sect. A Found. Adv. 76 (2020) 24–31, https://doi.org/10.1016/j.nanoen.2020.105052.

[231] H. Mutsuda, K. Kawakami, T. Kurokawa, Y. Doi, Y. Tanaka, A technology of electrical energy generated from ocean power using flexible piezoelectric device, (2010) 313–321. https://doi.org/10.1115/OMAE2010–20103.

[232] M. Ahmadian, R. Murray, M.N. Ghasemi-Nejhad, J. Rastegar, Novel two-stage piezoelectric-based ocean wave energy harvesters for moored or unmoored buoys, in: The 16th International Symposium on: Smart Structures and Materials & Nondestructive Evaluation and Health Monitoring, 2009.

[233] H.J. Hodges, J. Ruedy, L. Soede, M. Weber, J. Ruiz-Minguela, P. Jeffrey, H. Bannon, E. Holland, M. Maciver, R. Hume, D. Villate, J.-L. Ramsey, An International Evaluation and Guidance Framework for Ocean Energy Technology, 2021.

[234] P. Zeng, A. Khaligh, A permanent-magnet linear motion driven kinetic energy harvester, IEEE Trans. Ind. Electron. 60 (2013) 5737–5746, https://doi.org/10.1109/tie.2012.2229674.

[235] Z. Wang, J. An, J. Nie, J. Luo, J. Shao, T. Jiang, B. Chen, W. Tang, Z.L. Wang, A self-powered angle sensor at nanoradian-resolution for robotic arms and personalized medicare, Adv. Mater. 32 (2020), 2001466, https://doi.org/10.1002/adma.202001466.

[236] Y. Wang, H. Wu, L. Xu, H. Zhang, Y. Yang, Z.L. Wang, Hierarchically patterned self-powered sensors for multifunctional tactile sensing, Sci. Adv. 6 (2020) 9083, https://doi.org/10.1126/sciadv.abb9083.

[237] J. Tian, X. Chen, Z.L. Wang, Environmental energy harvesting based on triboelectric nanogenerators, Nanotechnology 31 (2020), 242001, https://doi.org/10.1088/1361-6528/ab793e.

[238] H. Tao, J. Gibert, Multifunctional mechanical metamaterials with embedded triboelectric nanogenerators, Adv. Funct. Mater. 30 (2020), 2001720, https://doi.org/10.1002/adfm.202001720.

[239] G.D. Bixler, B. Bhushan, Biofouling: lessons from nature, Philos. Trans. R Soc. 370 (2012) 2381–2417, https://doi.org/10.1098/rsta.2011.0502.

[240] M. Abbas, M. Shafiee, An overview of maintenance management strategies for corroded steel structures in extreme marine environments, Mar. Struct. 71 (2020), 102718, https://doi.org/10.1016/j.marstruc.2020.102718.

Dr. Xiu Xiao graduated from Tsinghua University in 2017. She was a visiting scholar at Purdue University during 2014–2016. Now she is an assistant professor in the Marine Engineering College, Dalian Maritime University. Her current research is mainly focused on new energy and its applications.

Prof. Yong Ma received his Ph.D. degree from Harbin Engineering University in 2013. Now he is a Professor in the School of Marine Engineering and Technology, Sun Yat-sen University. His current research is mainly focused on the floating structure hydrodynamic performance prediction, ocean energy devices, fluid dynamics testing technology and triboelectric nanogenerators.

Zhou Li is a Professor and Principal Investigator of Beijing Institute of Nanoenergy and Nanosystems (BINN) and School of Nanoscience and Technology, University of Chinese Academy of Sciences. He is also the director of Nanoenergy and Biosystem Lab in BINN. His research focused on self-powered medical electronics, implantable triboelectric nanogenerator (iTENG), bioabsorbable energy harvestor, biosensors and wearable medical devices. He was supported by the National Youth Talent Support Program and award "Young Investigator's Award" by International Federation for Medical and Biological Engineering (IFMBE).

Tiancong Zhao received the M.S. degree from the School of Dalian Maritime University, China., in 2017. He is currently pursuing the Ph.D. degree at Sun Yat-sen University, China. His research interests focus on energy harvesters.

Prof. Zhong Lin Wang received his Ph.D. degree from Arizona State University in Physics. He now is the Hightower Chair in Materials Science and Engineering, Regents' Professor at Georgia Tech, the chief scientist and director of the Beijing Institute of Nanoenergy and Nanosystems, Chinese Academy of Sciences. Prof. Wang has made original and innovative contributions to the synthesis, discovery, characterization and understanding of fundamental physical properties of oxide nanobelts and nanowires, as well as applications of nanowires in energy sciences, electronics, optoelectronics and biological science. His discovery and breakthroughs in developing nanogenerators establish the principle and technological road map for harvesting mechanical energy from environmental and biological systems for powering personal electronics. His research on self-powered nanosystems has inspired the worldwide efforts in academia and industry for studying energy for micro-nano-systems, which is now a distinct disciplinary in energy research and future sensor networks. He coined and pioneered the fields of piezotronics and piezophototronics by introducing piezoelectric potential gated charge transport process in fabricating new electronic and optoelectronic devices.

Prof. Minyi Xu received his Ph.D. degree from Peking University in 2012. During 2016–2017, he joined Professor Zhong Lin Wang' group at Georgia Institute of Technology. Now he is a Professor in the Marine Engineering College, Dalian Maritime University. His current research is mainly focused on the areas of blue energy, self-powered systems, triboelectric nanogenerators and its practical applications in smart ship and ocean.